

THE CRYSTAL CHEMISTRY OF STAUROLITE. III. LOCAL ORDER AND CHEMICAL COMPOSITION

FRANK C. HAWTHORNE¹, LUCIANO UNGARETTI, ROBERTA OBERTI, FRANCA CAUCIA
AND ATHOS CALLEGARI

CNR Centro di Studio per la Cristallografia e la Cristallografia, via Bassi 4, I-27100 Pavia, Italy

ABSTRACT

Vacancy (\square) – cation substitutions are important at several sites in the staurolite structure. Thus although the formula $[\text{Fe}_4\text{Al}_{18}\text{Si}_8\text{O}_{46}(\text{OH})_2]$ shows perfect agreement with Pauling's second rule in regard to its long-range structure, there are very large deviations at the local scale. The most probable local patterns of order in staurolite are derived using the structural information given by Hawthorne *et al.* (1993a), and a combination of stereochemical constraints. The probability of occurrence of each possible pattern of order is evaluated from its degree of agreement with the valence-sum rule (Brown 1981), for which the local bond-lengths were calculated for sites involved in the \square -cation substitutions. Summing over the more probable patterns of local order gives good agreement with the observed bulk-chemistry of staurolite. Moreover, the reason for the chemical complexity of staurolite becomes apparent. For the formula $\text{Fe}_4\text{Al}_{18}\text{Si}_8\text{O}_{46}(\text{OH})_2$, the local bond-valence distributions are poor; the structure needs 4 H pfu for a satisfactory local bond-valence distribution. However, the resulting formula $[\text{Fe}_4\text{Al}_{18}\text{Si}_8\text{O}_{46}(\text{OH})_4]^{2+}$ has a net positive charge. At the long-range level, such a charge cannot occur, and the principal heterovalent substitutions in staurolite [$\text{Al} \rightleftharpoons \text{Si}$; $\text{Mg} \rightleftharpoons \text{Al}$; $\square \rightleftharpoons \text{H}$; $\text{Li} \rightleftharpoons \text{Fe}^{2+}$, $\square \rightleftharpoons \text{Fe}^{2+}$] all act such as to reduce this charge. Thus we see the chemical complexity of staurolite as resulting from the interaction between long-range and short-range charge-balance requirements. Of particular importance in this regard is the occupancy of the $M(4A)$ and $M(4B)$ sites via the substitution $M^{(4)}\text{Fe}^{2+} + 2T^{(2)}\square \rightarrow M^{(4)}\square + 2T^{(2)}\text{Fe}^{2+}$ [$M^{(4)}\text{Fe}^{T(2)}\square_2 (M^{(4)}\square^{T(2)}\text{Fe}^{2+})_{-1}$] which reduces both the net charge and the number of cations in the structure below 30 apfu while maintaining an ideal local bond-valence distribution. The chemical composition of staurolite can be written as



where

A =	Fe ²⁺ , Mg, \square ($\square \geq 2$)	M(4A), M(4B)
B =	Fe ²⁺ , Zn, Co, Mg, Li, Al, Fe ³⁺ , Mn ²⁺ , \square	T(2)
C =	Al, Fe ³⁺ , Cr, V, Mg, Ti	M(1A), M(1B), M(2)
D =	Al, Mg, \square ($\square \geq 2$)	M(3A), M(3B)
T =	Si, Al	T(1)
X =	OH, F, O ²⁻	O(1A), O(1B)

The principal (heterovalent) end-members are:

(1)	□ ₄	Fe ₄ ²⁺	Al ₁₆	(Al ₂ □ ₂)	Si ₈	O ₄₀	[(OH) ₂ O ₆]
(2)	(□ ₂ Fe ₂ ²⁺)	□ ₄	Al ₁₆	(Al ₂ □ ₂)	Si ₈	O ₄₀	[(OH) ₆ O ₂]
(3)	□ ₄	Fe ₄ ²⁺	Al ₁₆	(□ ₄)	Si ₈	O ₄₀	[(OH) ₈]
(4)	□ ₄	Fe ₄ ²⁺	Al ₁₆	(Al ₂ □ ₂)	(Si ₄ Al ₄)	O ₄₀	[(OH) ₆ O ₂]
(5)	□ ₄	Fe ₄ ²⁺	(Al ₁₂ Mg ₄)	(Al ₂ □ ₂)	Si ₈	O ₄₀	[(OH) ₆ O ₂]
(6)	□ ₄	Li ₄	Al ₁₆	(Al ₂ □ ₂)	Si ₈	O ₄₀	[(OH) ₆ O ₂]

Homovalent end-members can be derived from these by the usual type of homovalent substitutions (*i.e.*, Zn → Fe²⁺, Co²⁺ → Fe²⁺, Mg → Fe²⁺).

Keywords: staurolite, chemical formula, bond valence, end members.

SOMMAIRE

Les substitutions impliquant cations et lacunes sont importantes dans plusieurs positions dans la structure de la staurolite. Malgré une concordance évidente avec la deuxième règle de Pauling dans la formule $\text{Fe}_4\text{Al}_{18}\text{Si}_8\text{O}_{46}(\text{OH})_2$ par rapport à la structure à longue échelle, il y a des écarts importants à courte échelle. Le schéma d'ordre local le plus probable découle de

¹Permanent address: Department of Geological Sciences, University of Manitoba, Winnipeg, Manitoba R3T 2N2.

l'information structurale de Hawthorne *et al.* (1993a) et une combinaison de contraintes stéréochimiques. Nous évaluons la probabilité de chaque schéma d'ordre possible en utilisant le degré de concordance à la règle de la somme des valences (Brown 1981); les longueurs de liaisons dans les situations locales ont été calculées pour les sites impliqués dans les schémas de substitution □ - cation. Une évaluation des schémas les plus probables d'ordre local permet d'obtenir une bonne concordance avec la composition globale de la staurolite. De plus, elle parvient à expliquer la complexité chimique de cette espèce. Dans le cas de la formule $\text{Fe}_4\text{Al}_{18}\text{Si}_8\text{O}_{46}(\text{OH})_2$, la distribution locale des valences de liaisons n'est pas satisfaisante; la structure requiert quatre atomes d'hydrogène par unité formulaire pour obtenir une distribution des valences de liaisons satisfaisante. Cependant, la formule qui en résulte, $[\text{Fe}_4\text{Al}_{18}\text{Si}_8\text{O}_{44}(\text{OH})_4]^{2+}$, possède une charge résiduelle positive. Devant l'impossibilité d'une telle charge à longue échelle, les diverses substitutions hétérovalentes [$\text{Al} = \text{Si}$, $\text{Mg} = \text{Al}$, $\square = \text{H}$, $\text{Li} = \text{Fe}^{2+}$, $\square = \text{Fe}^{2+}$] serviront à réduire cette charge. Nous voyons donc que la complexité chimique de la staurolite résulte de l'interaction entre les exigences de la balance des charges à courte et à longue échelles. Particulièrement important à cet égard est le degré d'occupation des sites $M(4A)$ et $M(4B)$ selon la substitution ${}^{M(4)}\text{Fe}^{2+} + 2{}^{T(2)}\square \rightarrow {}^{M(4)}\square + 2{}^{T(2)}\text{Fe}^{2+}$ [${}^{M(4)}\text{Fe}^{T(2)}_2$ (${}^{M(4)}\square$ ${}^{T(2)}\text{Fe}^{2+}_2$)]₁, qui réduit à la fois la charge totale et le nombre de cations à moins de 30 atomes par unité formulaire dans la structure tout en conservant une distribution locale idéale des valences de liaisons. On peut s'exprimer la composition chimique de la staurolite en ces termes:



Dans cette expression,

A =	Fe^{2+} , Mg, \square ($\square \geq 2$)	$M(4A)$, $M(4B)$
B =	Fe^{2+} , Zn, Co, Mg, Li, Al, Fe^{3+} , Mn^{2+} , \square	$T(2)$
C =	Al, Fe^{3+} , Cr, V, Mg, Ti	$M(1A)$, $M(1B)$, $M(2)$
D =	Al, Mg, \square ($\square \geq 2$)	$M(3A)$, $M(3B)$
T =	Si, Al	$T(1)$
X =	OH, F, O^{2-}	$O(1A)$, $O(1B)$

Les principaux pôles (hétérovalents) sont:

(1)	\square_4	Fe_4^{2+}	Al_{16}	$(\text{Al}_2\square_2)$	Si_8	O_{40}	$[(\text{OH})_2\text{O}_6]$
(2)	$(\square_2\text{Fe}_2^{2+})$	\square_4	Al_{16}	$(\text{Al}_2\square_2)$	Si_8	O_{40}	$[(\text{OH})_6\text{O}_2]$
(3)	\square_4	Fe_4^{2+}	Al_{16}	(\square_4)	Si_8	O_{40}	$[(\text{OH})_8]$
(4)	\square_4	Fe_4^{2+}	Al_{16}	$(\text{Al}_2\square_2)$	(Si_4Al_4)	O_{40}	$[(\text{OH})_6\text{O}_2]$
(5)	\square_4	Fe_4^{2+}	$(\text{Al}_{12}\text{Mg}_4)$	$(\text{Al}_2\square_2)$	Si_8	O_{40}	$[(\text{OH})_6\text{O}_2]$
(6)	\square_4	Li_4	Al_{16}	$(\text{Al}_2\square_2)$	Si_8	O_{40}	$[(\text{OH})_6\text{O}_2]$

On peut ensuite dériver les pôles homovalents au moyen des schémas conventionnels de substitution homovalente (*i.e.*, $\text{Zn} \rightarrow \text{Fe}^{2+}$, $\text{Co}^{2+} \rightarrow \text{Fe}^{2+}$, $\text{Mg} \rightarrow \text{Fe}^{2+}$).

(Traduit par la Rédaction)

Mots-clés: staurolite, formule chimique, valence de liaison, pôles.

INTRODUCTION

There has been significant progress in the last few years in unravelling the "enigma" of staurolite. Hawthorne *et al.* (1993a) reviewed the current state of knowledge of the structure and crystal chemistry, and presented site-scattering refinements for 42 staurolite crystals covering more or less the complete range of observed (natural) compositions. They showed that staurolite is monoclinic $C2/m$, with β varying over the range 90.00–90.45°. Variation in degree of Al- \square order over the $M(3A)$ and $M(3B)$ sites is coupled to the variation in the β angle; a detailed interpretation of this is given by Hawthorne *et al.* (1993b). Complete site-populations were assigned on the basis of site-scattering refinement, the results of electron- and ion-microprobe analyses, and a detailed consideration of overall (long-range) crystal-chemical relationships in the staurolite structure, especially the systematic variation in mean bond-length as a function of the mean radius of the constituent cations.

However, a full understanding of the chemical variations in staurolite requires knowledge of the local (short-range) order. There have been several proposals concerning patterns of local order in staurolite (Smith 1968, Holdaway *et al.* 1986b, Ståhl *et al.* 1988, Dyar *et al.* 1991), but these have lacked the comprehensive data necessary to confirm the general applicability of the ideas proposed. Here, we systematically examine the possible patterns of local order for the various compositional varieties of staurolite refined by Hawthorne *et al.* (1993a). The stability of possible patterns of local order is evaluated using bond-valence theory (Brown 1981).

STEREOCHEMICAL AND BOND-VALENCE CONSIDERATIONS

Various partial models for the ordering of cations and vacancies have been proposed in several previous studies. However, it is worthwhile to consider such ordering from as rigorous a viewpoint as possible,

such that the details of the arguments are explicitly stated and hence open to criticism or re-interpretation by others.

One of the problems associated with cation disorder is that the observed bond-lengths do not (usually) represent real bond-lengths, but bond-lengths averaged over all the patterns of local order in the crystal. The derivation of local (short-range, as distinct from long-range) stereochemistry is a very difficult problem. However, the special character of the cation-vacancy disorder in staurolite allows us to derive such information in a rather unusual way. As discussed in detail by Hawthorne *et al.* (1993b), staurolite can be considered as an order-disorder series; the end members are disordered orthorhombic staurolite, with $\beta = 90^\circ$, and fully ordered monoclinic staurolite, with $\beta = 90.64^\circ$. The Al - □ ordering over $M(3A)$ and $M(3B)$ and the Fe^{2+} - □ ordering over $M(4A)$ and $M(4B)$ both couple to the β angle; associated stereochemical parameters show a similar coupling, and consequently it is possible to extrapolate to the ordered monoclinic structure to derive actual bond-lengths for full and vacant sites.

The "kyanite" layer

First, we will consider that part of the structure that is reasonably independent of cation - □ ordering, essentially the $M(1A)$, $M(1B)$, $M(2)$ and $T(1)$ polyhedra. There is some substitution of Mg for Al at $M(1A)$ and $M(1B)$, and Al for Si at the $T(1)$ site. Although these substitutions cause some adjustment of bond lengths, the use of the universal curves of Brown (1981) to calculate bond valences takes this problem into account, as Mg, Al and Si belong to the same isoelectronic series of the periodic table. This approach is only an approximation, as it does not account for Mg-for-Al and Al-for-Si substitution; however, as the concentrations of these elements show only minor variation (in general) and do not seem to correlate strongly with the principal compositional variations, the approximation used should not introduce significant uncertainty into

the discussions. The resulting bond-valence arrangement for crystal S(1), sample 71-62R, is shown in Table 1. Some explanation of the superscripts and arrows should perhaps be given. Where no superscripts are given, the multiplicity of the incident bond is 1 in both directions; thus $T(1)$ bonds to one O(2A) atom, and O(2A) bonds to one $T(1)$ atom. Where superscripts and arrows are given, the multiplicity of the incident bond in the direction of the arrow is given by the superscript. Thus $M(1A)$ bonds to two O(2A) atoms, whereas O(2A) bonds to one $M(1A)$ atom; likewise, $M(2)$ bonds to one O(1A) atom, whereas O(1A) bonds to two $M(2)$ atoms. Anions O(2A), O(2B) and O(4) have their local bond-valence requirements approximately satisfied, with sums fairly close (± 0.1 valence units, v.u.) to the ideal value of 2.0 v.u. The bond-valence requirements of the anions O(1A), O(1B), O(3) and O(5) are not satisfied, and participate extensively in the bonding to the rest of the structure (the oxide-hydroxide layer); thus in considering local patterns of □-cation order in the oxide-hydroxide layer, we can focus solely on the O(1A), O(1B), O(3) and O(5) anions, and use the partial bond-valence sums from the $M(1A)$, $M(1B)$, $M(2)$ and $T(1)$ cations for all the patterns of □ - cation order considered.

$M(3A)$ and $M(3B)$ sites: bond-valence considerations

First it is necessary to derive bond lengths for the fully ordered monoclinic end-member. Using the ratio

TABLE 2. LOCAL BOND-VALENCE* ARRANGEMENTS AROUND OCCUPIED SITES IN STAUROLITE CRYSTAL S(1) (SAMPLE 71-62R)

M(3A)-M(3B) bond-valence distribution				
	M(3A)		M(3B)	
O(1A)	0.647 ^{2±} ↓			
O(2A)			0.657 ^{4±} ↓	
O(3)	0.423 ^{2±} ↓		0.420 ^{4±} ↓	
Sum	2.986		2.994	
M(4A)-M(4B) bond-valence distribution				
	M(4A)		M(4B)	
O(1A)	0.367 ^{2±} ↓			
O(1B)			0.387 ^{2±} ↓	
O(5)	0.295 ^{4±} ↓		0.307 ^{4±} ↓	
Sum	1.914		2.002	
H(1A)-H(1B) bond-valence distribution				
	H(1A)	H(1B)	H(2A)	H(2B)
O(1A)	0.78		0.92	0.08
O(1B)		0.78	0.08	0.92
O(3)	0.11 ^{2±} ↓	0.11 ^{2±} ↓		
Sum	1.00	1.00	1.00	1.00

* bond valences calculated from the parameters of Brown (1981).

TABLE 1. BOND-VALENCE ARRANGEMENT* IN THE "KYANITE" LAYER OF STAUROLITE CRYSTAL S(1), SAMPLE 71-62R

	M(1A)	M(1B)	M(2)	T(1)	Sum
O(1A)			0.477 ^{2±} →		0.954
O(1B)			0.479 ^{2±} →		0.958
O(2A)	0.467 ^{2±} ↓		0.481	0.968	1.916
O(2B)		0.465 ^{2±} ↓	0.488	0.969	1.922
O(3)			0.544	0.933	1.477
O(4)	0.510 ^{2±} ↓	0.505 ^{2±} ↓		0.945	1.960
O(5)	0.517 ^{2±} ↓	0.517 ^{2±} ↓	0.545		1.579
Sum	2.988	2.974	3.014	3.813	

* the superscripts are explained in the text

of the ideal mean bond-length to the observed mean bond-length [for example, $1.925 \div 1.973$ for $M(3A)$ in crystal S(1)], we can calculate (approximate) individual bond-lengths for complete Al occupancy of the $M(3A)$ site from the observed individual bond-lengths; this calculation should give us the local stereochemistry where $M(3A)$ is occupied by Al. This also was done for the $M(3B)$ site, and the resulting bond-valence arrangement for crystal S(1) is shown in Table 2.

Note that both $M(3A)$ and $M(3B)$ bond to the O(3) anion. For a local arrangement in which $M(3A)$ and $M(3B)$ are both occupied (by Al), O(3) receives an

aggregate bond-valence of $[1.477 + 0.423 + 0.420]$, *i.e.*, 2.32 v.u. This is considerably higher than the ideal value of 2.0 v.u., suggesting that $M(3A)$ and $M(3B)$ are not simultaneously occupied by Al at the local scale. Of course, some local arrangements of this sort *must* occur (except in a completely ordered monoclinic staurolite), as the bulk composition of the $M(3)$ sites is $[0.5 \text{ Al} + 0.5 \square]$; however, local ordering will strongly favor Al- \square associations, and the discussions of Hawthorne *et al.* (1993b) suggest some kind of domain structure based on Al - \square ordering at $M(3A)$ and $M(3B)$.

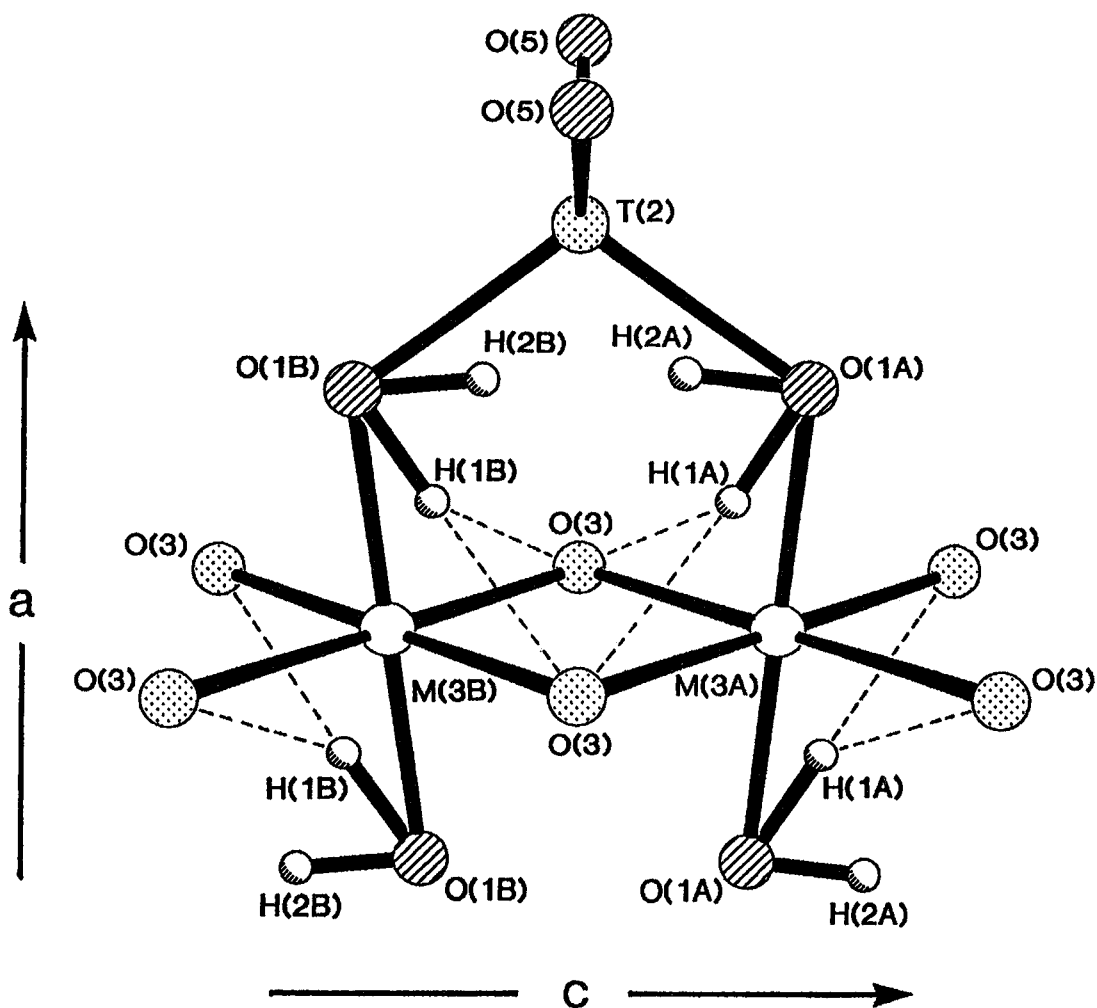


FIG. 1. The hydrogen and neighboring positions in staurolite (coordinates from Ståhl *et al.* 1988, site nomenclature from Hawthorne *et al.* 1993a). Hydrogen bonds are shown by broken lines; note that not all the positions shown can be occupied simultaneously. The primed and unprimed H positions belong to different local configurations.

TABLE 3. HYDROGEN ENVIRONMENTS IN STAUROLITE*

H(1A)-O(1A)**	1.009(5)	H(1B)-O(1B)	1.010(4)
H(1A)-O(3) x2	2.070(4)	H(1B)-O(3) x2	2.078(3)
O(1A)-O(3)	2.849(1)	O(1B)-O(3)	2.858(1)
O(1A)-H(1A)-O(3)	132.3(2)	O(1B)-H(1B)-O(3)	134.4
O(3)-H(1A)-O(3)	91.1(2)	O(3)-H(1B)-O(3)	90.6
H(2A)-O(1A)	0.90(3)	H(2B)-O(1B)	0.88(2)
H(2A)-O(1B)	2.32(3)	H(2B)-O(1A)	2.35(2)
O(1A)-O(1B)	3.215(2)	O(1B)-O(1A)	3.215(2)
O(1A)-H(2A)-O(1B)	174	O(1B)-H(2B)-O(1A)	170
H(2A)-O(3)	2.51	H(2B)-O(3)	2.56
O(1A)-H(2A)-O(3)	103	O(1B)-H(2B)-O(3)	101

* from Ståhl *et al.* (1988)

** distances in Å, angles in (°)

M(4A) and M(4B) sites: bond-valence considerations

Hawthorne *et al.* (1993a) showed that these sites are occupied by Fe²⁺ in nearly all samples of staurolite examined. The fact that partly occupied and vacant *M(4)* octahedra have the same size indicates that the observed bond-lengths are probably quite close to the local bond-lengths around an occupied *M(4A)* or *M(4B)* site. This argument is further supported by the sum of the constituent ionic radii (radii from Shannon 1976): $[^6\text{Fe}^{2+} + ^{3.5}\text{O}] = 0.78 + 1.37 = 2.15 \text{ \AA}$, equal to the mean bond-lengths at the *M(4)* sites in staurolite. Consequently, we can use the observed *M(4)*-O distances to calculate bond-valence distributions for local ordered arrangements. The results are shown in Table 2.

Both *M(4A)* and *M(4B)* bond to the O(5) anion. For a local arrangement in which *M(4A)* and *M(4B)* are both occupied (by Fe²⁺), O(5) receives an aggregate bond-valence of $[1.579 + 0.295 + 0.307] = 2.181 \text{ v.u.}$ This is higher than the ideal value of 2.0 v.u., but probably not sufficiently to consider this as an intrinsically unstable arrangement. Thus we will provisionally accept the possibility that *M(4A)* and *M(4B)* can be simultaneously occupied at the local level.

H(1A), H(1B), H(2A) and H(2B) sites: bond-valence considerations

Note that these sites have been relabeled (Hawthorne *et al.* 1993a) relative to earlier studies (especially that of Ståhl *et al.* 1988) such that O(1A) is the hydrogen-bond donor associated with H(1A) and H(2A), and O(1B) is the hydrogen-bond donor associated with H(1B) and H(2B) (Fig. 1). The assignment of hydrogen-bond valences is a difficult matter (Brown 1976a, b, 1981, Brown & Altermatt 1985). Hydrogen-bonding has very strong directional charac-

ter, and also is sensitive to the bond angles involved; consequently, a single bond-valence relationship is very difficult (if not impractical) to produce. This is particularly the case in staurolite. Local stereochemical details for the H positions are shown (Table 3) for the neutron-diffraction refinement of the structure given by Ståhl *et al.* (1988).

The H(1A) and H(1B) environments are very similar, and can be assigned the same bond-valence distributions; the discussion given here is for the H(1A) atom. H(1A) forms a bifurcated hydrogen-bond with two O(3) anions. We have assigned to H...O(3) a bond valence of 0.11 v.u.; as there are two hydrogen-bonds, the O(1A)-H bond-valence is thus 0.78 v.u., a reasonable value for an O-H distance of 1.01 Å.

The H(2A) site is 2.3 Å from O(1B). Although this distance is longer than that commonly considered to be relevant for significant bonding interaction, Brown (1976b) has shown that such weak interactions are significant; here we assign a strength of 0.08 v.u. to this bond. The resultant O(1A)-H(2A) bond-valence is 0.92 v.u., again a reasonable value for the observed distance of 0.90 Å. A similar argument may be given for the H(2B) site. The O(1A)-H(2A) and O(1B)-H(2B) distances are significantly longer (Table 3), and the O(1A)-H(2A)-O(3) and O(1B)-H(2B)-O(3) angles of ~102° are much smaller than those normally involved in hydrogen bonding; this indicates that there is no hydrogen-bonding interaction between H(2A), H(2B) and O(3).

The resultant bond-valence distributions are shown in Table 2. Both H(1A) and H(2A) bond strongly to the O(1A) anions. If both H(1A) and H(2A) were locally occupied, the resultant bond-valence sum at O(1A) would be 2.654 v.u. This is far higher than the ideal value of 2.0 v.u., and indicates that H(1A) and H(2A) cannot be simultaneously occupied at the local scale. Similarly H(1B) and H(2B) cannot be simultaneously occupied. Note that this also means that only OH⁻ [and not (H₂O)⁰] can occupy the O(1A) and O(1B) positions in staurolite.

Constraints resulting from cation-cation approaches

Some of the geometrically possible local arrangements of cations and vacancies in staurolite can be discounted because they produce cation-cation separations that are far too short to be stable. Important distances in this regard are listed in Table 4. The implications for these configurations are now discussed for each site (or group of sites) in turn.

M(3A) and M(3B): If *M(3A)* is occupied, the neighboring H(1A) site is vacant. The question of the *M(3A)*-H(2A) approach of 2.04 Å is a little less clear. As shown in Table 4, there are H(1A)-*M(2)* and H(1B)-*M(2)* separations of 2.46 Å. As *M(2)* is completely occupied by cations, this must be a stable *M...H*

TABLE 4. CLOSE CATION-CATION APPROACHES (Å) IN STAUROLITE

M(3A)-H(2A)	2.04	M(3B)-H(2B)	2.08
M(4A)-T(2)	1.64	M(4B)-T(2)	1.64
M(4A)-H(2A)	2.14	M(4B)-H(2B)	2.08
T(2)-H(1A)	2.37		
T(2)-H(1B)	2.37		
T(2)-H(2A)	1.38		
T(2)-H(2B)	1.36		
T(2)-M(4A)	1.64		
T(2)-M(4B)	1.64		
H(1A)-M(3A)	1.04	H(1B)-M(3B)	1.05
H(1A)-H(1A)	2.09	H(1B)-H(1B)	2.10
H(1A)-H(1B)	2.16	H(1B)-H(1A)	2.16
H(1A)-H(2A)	0.99	H(1B)-H(2B)	1.03
H(1A)-H(2B)	2.06	H(1B)-H(2A)	2.01
H(1A)-M(2)	2.46	H(1B)-M(2)	2.46
H(2A)-M(3A)	1.05	H(2B)-M(3B)	2.08
H(2A)-M(4A)	2.14	H(2B)-M(4B)	2.08
H(2A)-H(1B)	2.01	H(2B)-H(1A)	2.06
H(2A)-T(2)	1.38	H(2B)-T(2)	1.36
H(2A)-H(1A)	0.99	H(2B)-H(1B)	1.03
H(2A)-H(2B)	1.45	H(2B)-H(2A)	1.45

distance in staurolite. As discussed later, there are $T(2)$ -H separations of 2.37 Å that also must occur. However, the longest M-O distances observed locally are ~1.98 Å, and it is generally considered that cations will not approach other cations more closely than the bonded anions. Consequently, there is some value in the range 1.98-2.37 Å closer than which the hydrogen atom will not approach the cation. In well-ordered structures, hydrogen is normally separated from other cations (except for the well-known H-H approach of 1.4 Å in the H₂O group) by at least 2.3 Å, and so we will take this as our limit of stability. Hence if $M(3A)$ is occupied, both neighboring H(1A) and H(2A) sites are vacant.

M(4A) and M(4B): If $M(4A)$ or $M(4B)$ are occupied, the adjacent $T(2)$ site must be vacant because of the close $M(4)$ - $T(2)$ approach across the shared face; this is the case no matter what cations occupy either site, as 1.64 Å is shorter than any of the expected cation-anion distances for the cations occupying either site. These arguments are not materially affected by the positional disorder at the $T(2)$ site. Also, if $M(4A)$ is occupied, the adjacent H(2A) site must be vacant, and if $M(4B)$ is occupied, the adjacent H(2B) site must be vacant.

T(2) site: If the $T(2)$ site is occupied, the stoichiometry of staurolite forces us to conclude that H(1A) or H(1B) (or both) are occupied (from the neutron-diffraction refinement of the structure of Ståhl *et al.* 1988), and thus a $T(2)$ -H approach of 2.37 Å must be a stable

arrangement. However, if $T(2)$ is occupied, the adjacent H(2A), H(2B), $M(4A)$ and $M(4B)$ sites are all vacant.

H(1A) and H(1B): If H(1A) is occupied, the adjacent $M(3A)$ site is vacant, and the same applies to H(1B) and $M(3B)$; all other close approaches concern H-H distances (Table 4), some having interesting stoichiometric implications. Consequently, before we can evaluate the restrictions of close H-H approaches on patterns of local order or mineral stoichiometry, it is necessary to decide what is an "unacceptable" H-H distance in a stable structure.

Ståhl *et al.* (1988) have listed H-H approaches of up to 2.16 Å that they consider as "too close for simultaneous occupancy". Although such questions are difficult to judge, we suggest that this distance is not a realistic limit, primarily from an examination of H-H approaches in well-ordered structures refined by neutron diffraction. Specifically, in deuterated hydrogarnet Ca₃Al₂(O₄D₄)₃ (Lager *et al.* 1987), the D-D approach is 1.95 Å, indicating that such separations are not intrinsically unstable.

Another factor that indicates that such distances are stable is the relative occupancies of the four H positions found by Ståhl *et al.* (1988). The O(1B) anions occupy two *trans* vertices of the $M(3B)$ octahedron. The corresponding H(1B)-H(1B) distance across the octahedron is 2.16 Å. If this approach is forbidden, with only one H(1B) position allowed to be occupied in any $M(3B)$ octahedron occupied by a vacancy, then the occupancy of the H(1B) position could not exceed half the vacancy at the $M(3B)$ site. This is not the case for the neutron-diffraction refinement of the staurolite structure by Ståhl *et al.* (1988). In this crystal, the vacancy at $M(3B)$ is 0.548(12), and the H(1B) occupancy is 0.380(12) as compared with 0.29, the maximum possible occupancy if the H(1B)-H(1B) approach of 2.16 Å is forbidden. Thus we consider H-H approaches of ~2.0 Å to be allowed.

As a result of the above arguments, all the H(1A)-H and H(1B)-H approaches of ~2.0 Å listed in Table 4 are considered as allowed. The only obviously unstable approaches are the H(1A)-H(2A) and H(1B)-H(2B) distances of ~1 Å that we have already designated as unstable on bond-valence grounds.

H(2A) and H(2B): If H(2A) is occupied, the adjacent $M(3A)$ site must be vacant [see above section on $M(3A)$ and $M(3B)$], and similarly for H(2B) and $M(3B)$; note that this is also in accord with the fact that H(1A) and H(2A) cannot be simultaneously locally occupied, either attached to the same O(1A) atom or to *trans* O(1A) atoms of the same local $M(3A)$ octahedron. We have decided above that an H(2A)- $M(4A)$ distance of 2.14 Å is unstable, and therefore if H(2A) is occupied, the adjacent $M(4A)$ must be empty. Also,

if H(2A) is occupied, then the adjacent T(2) is vacant. The H(2A)–H(2B) distance of 1.45 Å is probably not stable (such H–H distances only being seen in H₂O groups), and thus if H(2A) or H(2B) is occupied, the adjacent T(2) site is vacant.

Bond-valence arrangements for patterns of local order

Combination of preliminary bond-valence arrangements and constraints imposed by cation–cation interaction produces a fairly small number of possible patterns of local order. The relative probability of these may be evaluated by calculating the root-mean-square (RMS) deviation from ideality for the bond-valence sums around the anions. However, it is necessary to stress that the mean (*i.e.*, long-range average) lengths of each individual bond are not adequate for this procedure, especially where the substitutions at the cation sites involve vacancies. Consequently, it is necessary to derive “reasonable” local distances for fully ordered local arrangements. This has been done above for the M(3A), M(3B), M(4A) and M(4B) sites. The problem remains for the T(2) site. For this site, with its variety of substituent cations, variable vacancies and complex positional disorder, it is perhaps unrealistic to expect to be able to derive local stereochemistry. As a first attempt, we use Pauling bond-strengths for both divalent or monovalent occupancy of T(2).

Hydrogen-rich staurolite, M(3) occupied: The results for all patterns of local order chosen are shown in Table 5. There are six arrangements of approximately

equal RMS deviation from ideality; these are labeled (1) to (6) in Table 5. Arrangements (1) and (2) are what one might call the “normal” arrangements for staurolite, in which the T(2) site is occupied and adjacent M(4A) and M(4B) sites are vacant; complete bond-valence arrangements for these two patterns of order are shown in Table 6. The two next patterns [(3) and (4)] have the T(2) site vacant, and M(4A) and H(2B) [also M(4B) and H(2A)] occupied. The bond-valence arrangements for these patterns of order also are shown in Table 6. It is possible that we have overestimated the strength of the hydrogen bonds involving H(2A) and H(2B). If this is the case, then for the arrangements in which H(2A) and H(2B) are occupied, the root-mean-square deviations are reduced (to 0.081 in the extreme case of no hydrogen-bonding), whereas for the other patterns of Table 5, the root-mean-square deviations get larger. These patterns of local order correspond to the arrangement in the proposed structural domains 1A, 1B, 2A and 2B of Ståhl *et al.* (1988); however, at the moment, we suggest them only as local arrangements. Patterns (5) and (6) involve simultaneous occupancy of M(4A) and M(4B). In general, these patterns do not occur because of stoichiometric restrictions (see later discussion), but are found in Mg-rich staurolite S(41). Note that some of the bond-valence arrangements given in Table 6 can be improved by considering local models for the occupancy and environment of the T(2) site; this will be done later.

Hydrogen-rich staurolite, M(3) vacant: Each of the schemes of local order shown in Table 5 have one feature in common: they all involve one hydrogen atom. If we sum over all the schemes of local order, we end up with the M(3) sites on average exactly half-filled, and a hydrogen content of 4 apfu. However, Hawthorne *et al.* (1993a) show that the aggregate M(3) cation populations vary in the range 1.75–2.08 apfu, and Holdaway *et al.* (1986a) have shown that the hydrogen content of hydrogen-rich staurolite samples does exceed 4 apfu. Inspection of the site-scattering results for staurolite 71–62R (with an analyzed hydrogen content of 4.16 apfu) shows the total cation population of M(3) to be significantly less than 2.0 apfu. A total M(3) cation population of less than 2.0 apfu means that there must be some local structural configurations in which both M(3A) and M(3B) are vacant. The bond-valence consequences of this are examined in Table 7. According to Table 1, O(1A), O(1B), and O(3) are deficient in incident bond-valence. The only way in which this can be compensated is to have both H(1A) and H(1B) occupied. As is apparent from Table 7, there is still a significant bond-valence deficiency at O(3), which has a bond-valence sum of ~1.70 v.u. This situation can be alleviated by increasing the strength of the hydrogen bonding from H(1A) and H(1B) to O(3) [to 0.25 v.u.]. If the bond-valence

TABLE 5. POSSIBLE PATTERNS OF LOCAL ORDER IN STAUROLITE, TOGETHER WITH R.M.S. (ROOT-MEAN-SQUARE) DEVIATIONS FROM IDEALITY

	Local arrangement	R.M.S. deviation
(1)	*M(3A)–T(2)–H(1B)	0.095
	M(3A)–T(2)–H(2B)	0.141
	M(3A)–M(4A)–H(1B)	0.105
(3)	*M(3A)–M(4A)–H(2B)	0.091
	M(3A)–M(4B)–H(1B)	0.140
	M(3A)–M(4B)–H(2B)	0.159
(5)	M(3A)–M(4)–H(1B)	0.125
	M(3A)–M(4)–H(2B)	0.097
	M(3A)–[]–H(2B)	0.208
(2)	*M(3B)–T(2)–H(1A)	0.096
	M(3B)–T(2)–H(2A)	0.142
	M(3B)–M(4A)–H(1A)	0.135
	M(3B)–M(4A)–H(2A)	0.140
	M(3B)–M(4B)–H(1A)	0.103
(4)	*M(3B)–M(4B)–H(2A)	0.091
(6)	M(3B)–M(4)–H(1A)	0.094
	M(3B)–M(4)–H(2A)	0.123
	M(3B)–[]–H(2A)	0.207

TABLE 6. LOCAL BOND-VALENCE* ARRANGEMENTS** FOR THE FOUR MOST STABLE PATTERNS OF LOCAL ORDER (TABLE 5) FOR CRYSTAL S(1), SAMPLE 71-62R

(1)	M(3A)	T(2)	H(1B)	Sum	(2)	M(3B)	T(2)	H(1A)	Sum
O(1A)	0.647 ^{±2} ↓	0.50		2.101	O(1A)		0.50	0.78	2.23
O(1B)		0.50	0.78	2.238	O(1B)	0.657 ^{±2} ↓	0.50		2.11
O(3)	0.423 ^{±4} ↓		0.11 ^{±2} ↓	2.010	O(3)	0.420 ^{±4} ↓		0.11 ^{±2} ↓	2.00
O(5)		0.50 ^{±2} ↓		2.079	O(5)		0.50 ^{±2} ↓		2.07
Sum	2.986	2.00	1.00		Sum	2.994	2.00	1.00	

(3)	M(3A)	M(4A)	H(2B)	Sum	(4)	M(3B)	M(4B)	H(2A)	Sum
O(1A)	0.647 ^{±2} ↓	0.367 ^{±2} ↓	0.08	2.048	O(1A)			0.92	1.87
O(1B)			0.92	1.878	O(1B)	0.657 ^{±2} ↓	0.387 ^{±2} ↓	0.08	2.08
O(3)	0.423 ^{±4} ↓			1.900	O(3)	0.420 ^{±4} ↓			1.89
O(5)		0.295 ^{±4} ↓		1.874	O(5)		0.307 ^{±4} ↓		1.88
Sum	2.986	1.914	1.00		Sum	2.994	2.002	1.00	

* calculated with the curves of Brown (1981);

** these arrangements can be combined with the bond-valence arrangement of Table 1 to give the complete bond-valence arrangement throughout the (locally ordered) structure.

arrangement shown in parentheses in Table 7 is adopted, the bond-valence sums at all anions are reasonable. The donor-hydrogen interaction is weaker than is usually the case, but interactions of this type are found in crystals. Consequently, the pattern of local order of Table 7 seems realistic. It also is the only way in which more than 4 H apfu can be incorporated into the staurolite structure.

Normal staurolite: For these crystals (with H ≈ 3 apfu), there must be configurations of local order in which all H positions (*i.e.*, the unprimed positions of Fig. 1) are unoccupied; moreover, these must account for ~1/4 of the local configurations for the crystals to have the correct stoichiometry [for H = 4, H(1B) is fully occupied, and there are no H-free configurations; for H = 2, H(1B) is half occupied, and half of the configurations are H-free; for H = 3, H(1B) is three-quarters occupied, and one quarter of the configurations are H-free]. First, M(3A) and M(3B) cannot be simultaneously occupied at the local scale to compensate for

the lack of H, because our refinement results show M(3) to be half-occupied, and significant simultaneous occupancy of M(3A) and M(3B) would give M(3) occupancies much greater than 1.0 [*i.e.*, M(3A) + M(3B) >> 1]. Thus only one of the two M(3) sites can be occupied in the hydrogen-free configuration.

As shown above, ~1/4 of the local configurations do not involve hydrogen in normal staurolite. As an M(4A) or M(4B) site forms a local configuration in each of the adjacent M(3A)-M(3B) chains (Fig. 2), the participation of an occupied M(4A) or M(4B) site in the H-free configuration requires an aggregate M(4) occupancy of ~0.5 apfu; any local coupling will increase this value, and participation of both M(4A) and M(4B) in the local H-free configuration would result in 1.0 apfu at M(4). Inspection of the refined site-scattering at M(4A) and M(4B) (Hawthorne *et al.* 1993a) shows that none of these cases is possible. The aggregate M(4) site-scattering values are in the range 0.0-3.5 epfu, not compatible with either 0.5 or 1.0 apfu at M(4), given that the possible occupants of the M(4) sites are Fe and Mg. Thus occupied M(4) sites cannot be involved in the H-free configurations in normal staurolite.

There is only one possible remaining arrangement: the T(2) site must be occupied. The resulting bond-valence arrangement is shown in Table 8. With the T(2)-O bond valences used above, the bond-valence sums around the anions are satisfactory, with the notable exception of O(1B); the relevant sum here is 1.458 v.u., an obviously inadequate value. This anomaly is really not surprising, as this pattern of local order is the same as the M(3A)-T(2)-H(1B) pattern (1) of Tables 5 and 6, except that the H(1B) site is vacant. However, there seems to be no alternative to the arrangement, and so the structure *must* locally accom-

TABLE 7. LOCAL BOND-VALENCE* ARRANGEMENTS** FOR THE MOST STABLE LOCAL ORDERING PATTERN INVOLVING VACANT M(3) SITES

	T(2)	H(1A)	H(1B)	Sum
O(1A)	0.50	0.78(0.50) ^{±2} →		2.234 (1.954)*
O(1B)	0.50		0.78(0.50)	2.238 (1.954)
O(3)		0.11(0.25) ^{±2} ↓	0.11(0.25) ^{±2} ↓	1.697 (1.977)
O(5)	0.50 ^{±2} ↓			2.079
Sum	2.00	1.00	1.00	

* calculated with the curves of Brown (1981);

** these arrangements can be combined with the bond-valence arrangement of Table 1 to give the complete bond-valence arrangement throughout the (locally ordered) structure;

* for the significance of the values in parentheses, see text.

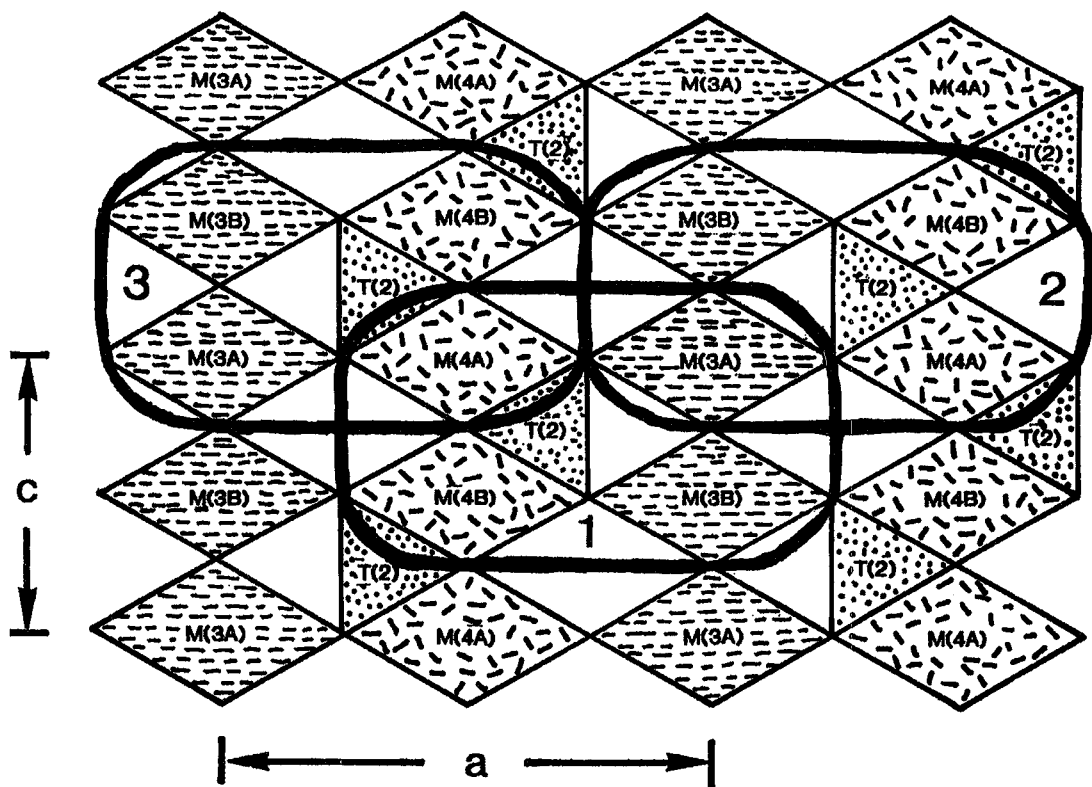


FIG. 2. An example of arrangements of local order in the staurolite structure, showing how one arrangement is not independent of the adjacent arrangements.

modate to this situation. How is this done? It cannot be by variable site-populations (*i.e.*, substitution of Mg for Al, or even Al for Fe^{2+}), as none of these show sufficient substitution to account for 1 H apfu. Consequently, it *must* be accommodated by variations at the $T(2)$ site. Again, the $T(2)$ site is occupied predominantly by divalent cations, and thus the accommodation for reduced bond-valence at $O(1B)$ cannot be compositional, except possibly on a minor scale. The only alternative is for the $T(2)$ cation to move toward $O(1B)$ [or $O(1A)$ in the alternate configuration] to increase the valence of this bond. *Here is obviously one of the driving forces for positional disorder at the $T(2)$ site.* It is difficult to give a quantitative idea of the local stereochemistry in this case. However, we note that

- (i) one of the $T(2)$ subsites is displaced toward the $M(3A)$ – $M(3B)$ chain;
- (ii) the $O(1A)$ and $O(1B)$ anions show strong anisotropic displacement parameters, with large U_{11} values, whereas the other anions are all fairly isotropic.

Thus it seems reasonable to propose that not only does the $T(2)$ cation locally move toward the

$M(3A)$ – $M(3B)$ chain, but also the $O(1A)$ and $O(1B)$ anions move toward $T(2)$ to produce very short $T(2)$ – $O(1A)$ or $T(2)$ – $O(1B)$ bonds at the local scale [in this regard, note that $O(3)$ also shows this anisotropic displacement, consistent with the local stereochemical model proposed above].

TABLE 8. LOCAL BOND-VALENCE* ARRANGEMENT** FOR THE MOST STABLE PATTERN OF LOCAL ORDER INVOLVING NO HYDROGEN

	*M(3A)	T(2)	Sum
O(1A)	0.647 ^{±2} ↓	0.50	2.101
O(1B)		0.50	1.458
O(3)	0.423 ^{±4} ↓		1.900
O(5)		0.50 ^{±2} ↓	2.079
Sum	2.986	2.00	

* calculated with the curves of Brown (1981);

** these arrangements can be combined with that of Table 1 to give the complete arrangement;

* there is an analogous arrangement involving $M(3B)$.

TABLE 9. LOCAL BOND-VALENCE* ARRANGEMENT** FOR THE MOST STABLE PATTERN OF LOCAL ORDER INVOLVING Li

	M(3A)	T(2)	H(1B)	Sum		M(3A)	T(2)	H(2B)	Sum
O(1A)	0.647 ^{±0.2} ↓	0.25		1.851	O(1A)		0.25	0.08	1.93
O(1B)		0.25	0.78	1.988	O(1B)	0.647 ^{±0.2} ↓	0.25	0.92	2.12
O(3)	0.423 ^{±0.4} ↓		0.11 ^{±0.2} ↓	2.010	O(3)	0.423 ^{±0.4} ↓			1.90
O(5)		0.25 ^{±0.2} ↓		1.829	O(5)		0.25 ^{±0.2} ↓		1.82
Sum	2.986	1.00	1.00		Sum	2.986	1.00	1.00	

* calculated with the curves of Brown (1981);

** these arrangements can be combined with the bond-valence arrangement of Table 1 to give the complete bond-valence arrangement throughout the (locally-ordered) structure;

* there are analogous arrangements involving M(3B).

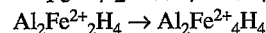
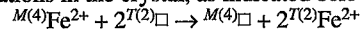
Li-bearing staurolite: From the stoichiometry and refined site-scattering in Li-rich staurolite (Hawthorne *et al.* 1993a), M(3A) or M(3B) must be occupied by Al, and T(2) by Li. This leaves a bond-valence deficiency at O(1B) or O(1A) that must be compensated by occupancy of H(1B) or H(2B) or H(1A) or H(2A). The resulting bond-valence arrangements are shown in Table 9, and the RMS deviations from ideality are 0.096 and 0.104, respectively, for occupancy of M(3A). These deviations suggest that the configuration with H(1B) is to be preferred, although there is no experimental evidence to support this point.

WHY ARE M(4A) AND M(4B) OCCUPIED?

In a previous section, we derived the patterns of local order that occur in staurolite; the bulk composition of the crystal is equal to the sum of all the local configurations over the whole volume of the crystal. In this regard, one local configuration is not independent of the adjacent configuration, as some of the sites belong to both configurations. This point may be seen by referring to Figure 2. A specific M(3A) site belongs to configuration 1 and configuration 2; similarly, a specific M(4A) site belongs to configuration 1 and configuration 3. Conversely, configurations 1, 2 and 3 each involve their own specific T(2) site. Thus in

summing over the local patterns to get the bulk composition of the crystal, the effective multiplicities of the local sites must be incorporated into the calculation. For M(3A), M(3B), M(4A) and M(4B), this value is 0.5; for T(2), H(1A), H(1B), H(2A) and H(2B), it is 1.0.

Let us consider a crystal made up of equal amounts of patterns 1 and 2 (Table 5), and focus on the cations of the oxide-hydroxide layer; the sum over both patterns is shown in Table 10. In terms of sites, the sum is M(3)₂T(2)₄H(1)₄ after allowing for the equipoint rank of each site; with M(3) = Al, T(2) = Fe²⁺ and H(1) = H, this gives a composition of Al₂Fe₄H₄. Now let us consider a crystal made up of equal amounts of local patterns 3 and 4 (Table 5). The analogous sum (Table 10) is M(3)₂M(4)₂H(2)₄; with M(3) = Al, M(4) = Fe²⁺ and H(2) = H, the composition is Al₂Fe₂H₄. We see immediately the effect of M(4) occupancy as compared with T(2) occupancy. Both patterns produce local bond-valence satisfaction, but have very different effects on the overall stoichiometry. Substitution of Fe²⁺ (or any other divalent cation) at M(4) rather than at T(2) reduces the total number of divalent cations in the crystal, as indicated below:



Thus M(4) occupancy is an effective mechanism for reducing the total cation charge of the crystal while maintaining bond-valence satisfaction at the local scale. As we will see later, the need to reduce the total cation charge in staurolite is the reason for the compositional and structural complexities of this mineral.

TABLE 10. CATION SUMS IN HYDROXIDE LAYER FROM SUMMING OVER PATTERNS OF LOCAL ORDER [(1)+(2)] AND [(3)+(4)]

(1) = M(3A)-T(2)-H(1B)	(2) = M(3B)-T(2)-H(1A)
(1) + (2) = M(3A) _{1/2} T(2)H(1B) + M(3B) _{1/2} T(2)H(1A)	
= M(3A) _{1/2} M(3B) _{1/2} T(2) ₂ H(1A)H(1B) = M(3)T(2) ₂ H(1) ₂	
Composition per formula unit = M(3) ₂ T(2) ₂ H(1) ₂ = Al ₂ Fe ₂ H ₄	
(3) = M(3A)-M(4A)-H(2B)	(4) = M(3B)-M(4B)-H(2A)
(3) + (4) = M(3A) _{1/2} M(4A) _{1/2} H(2B) + M(3B) _{1/2} M(4B) _{1/2} H(2A)	
= M(3A) _{1/2} M(3B) _{1/2} M(4A) _{1/2} M(4B) _{1/2} H(2A)H(2B)	
Composition per formula unit = M(3) ₂ M(4) ₂ H(2) ₂ = Al ₂ Fe ₂ H ₄	

POSITIONAL DISORDER AT THE T(2) SITE

As discussed by Hawthorne *et al.* (1993a), we were unable to satisfactorily resolve the positional disorder at the T(2) site. Solutions obtained from the refinement were dependent on the starting parameters, indicating that the refinements were converging on false minima; consequently, the solutions obtained cannot be considered as reliable. In spite of this, we can get a

semiquantitative idea of what is happening from the ranges of solutions obtained for the same samples of staurolite with crystals of different β angles (thus removing any possible compositional effects). As an example, we discuss the results for staurolite 117189.

Trends in $T(2)$ positional disorder

From the same starting parameters, we get reasonably consistent positions and site scatterings for the four crystals S(11), S(12), S(13) and S(14) of staurolite 117189. Although we cannot attach significance to the absolute values of the refined parameters, the trends as a function of β are significant, as they are similar to the solutions obtained from other refinements of the same data starting from different initial parameters for the $T(2)$ subsites. With $\beta \approx 90^\circ$, the positions approximate mirror symmetry through $z \approx 1/4$. The z parameter of $T(2c) \approx 1/4$, $T(2a)$ and $T(2b)$ are approximately equal distances either side of $z = 1/4$ (mean $z = 0.2496 \approx 1/4$); the x parameters of $T(2a)$ and $T(2b)$ are slightly different, but the difference is within the range of different solutions obtained with different starting models. Thus it seems reasonable to conclude that at $\beta = 90^\circ$, the $T(2)$ site disorder obeys long-range orthorhombic symmetry.

With increasing β , both $T(2a)$ and $T(2b)$ move toward decreasing values of z (Fig. 2); the x parameters also increase on average, but this may be within the variation of the false-minima solutions, and so we do not place much weight on this observation. Conversely, the z parameter of $T(2c)$ is almost constant at $\sim 1/4$ (0.249–0.250), with a small movement along x that again may not be significant. Thus a general pattern does emerge. If $\beta = 90^\circ$, the pattern of disorder has spatial orthorhombic symmetry. With increasing β , $T(2c)$ remains in approximately the same position, whereas $T(2a)$ and $T(2b)$ move along z such that their z parameter decreases. Unfortunately, we cannot derive any accurate idea of the behavior of the relative site-populations because of the high correlation between site scattering and the distance from the central site (*cf.* Alexander 1989). However, in difference-Fourier maps calculated with a central $T(2)$ site only, we noticed that the relative densities at the $T(2a)$ and $T(2b)$ subsites were systematically related to the β angle of the crystal. With increasing β , the $T(2a)$ position had increasing residual density, whereas the $T(2b)$ position had decreasing residual density. This finding suggests that the relative populations of the $T(2A)$ and $T(2B)$ positions are coupled to the spontaneous strain (Hawthorne *et al.* 1993b); however, note that they show the inverse coupling to that shown by $M(3A)$ – $M(3B)$ and $M(4A)$ – $M(4B)$, and parallel the proposed H – □ ordering over the H(1A) and H(1B) positions. This coupling suggests that the positional disorder at the $T(2)$ site is related to the various schemes of local order that develop in the oxide–hydroxide layer,

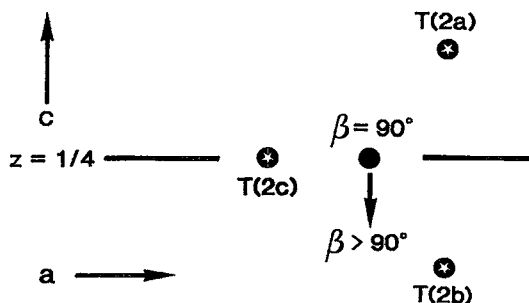


FIG. 3. Diagrammatic representation of the positional disorder at the $T(2)$ site in staurolite, showing the relative positions of the $T(2a)$, $T(2b)$ and $T(2c)$ positions (three-site model). The filled circle shows the position of the central $T(2)$ site (one-site model) at $\beta = 90^\circ$, and the arrow shows the locus of the z coordinate with increasing β angle for staurolite 117189 [crystals S(11–14) of Hawthorne *et al.* 1993a].

and is in line with our previous arguments concerning bond-valence distributions in patterns of local order.

The “central $T(2)$ -site” model

As we can only have confidence in the quantitative

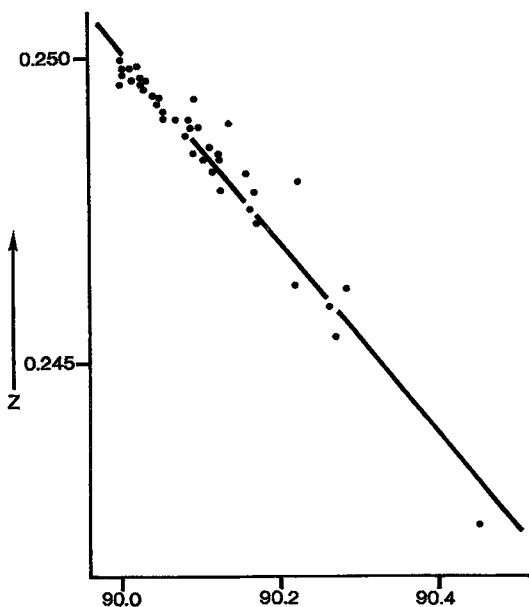


FIG. 4. Variation in z coordinate of the central $T(2)$ site with variation in β angle for the 42 crystals of staurolite refined by Hawthorne *et al.* (1993a).

TABLE 11. PAULING BOND-STRENGTH TABLE FOR A DISORDERED IDEAL STAUROLITE*

	M(1A)	M(1B)	M(2)	T(1)	M(3A)	M(3B)	M(4A)	M(4B)	T(2)	H(1A)	H(1B)	H(2A)	H(2B)	Sum
O(1A)			1/2 ²⁺		1/4 ²⁺		-	-	1/2	1/4				2
O(1B)			1/2 ²⁺			1/4 ²⁺			1/2		1/4		-	2
O(2A)	1/2 ²⁺		1/2	1										2
O(2B)		1/2 ²⁺	1/2	1										2
O(3)			1/2	1	1/4 ²⁺	1/4 ²⁺								2
O(4)	1/2 ²⁺	1/2 ²⁺		1										2
O(5)	1/2 ²⁺	1/2 ²⁺	1/2				-	-	1/2 ²⁺					2
Sum	3	3	3	4	1.5	1.5	-	-	2	1/4	1/4	-	-	

* note that this table is for the disordered long-range structure, not a local arrangement.

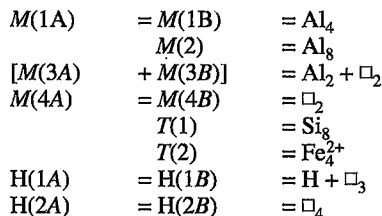
results of the central $T(2)$ site refinement, it is desirable to see if the disorder behavior deduced above has any discernible effect on the central $T(2)$ site results. Fortunately, this is the case. The results of the central $T(2)$ site-scattering refinements for crystals S(11), S(12), S(13) and S(14) are shown qualitatively in Figure 3. Where $\beta = 90^\circ$, $z \approx 1/4$; with increasing β , the x parameter of $T(2)$ remains essentially constant, whereas the z parameter gradually decreases, reflecting the actual behavior of the $T(2a)$ and $T(2b)$ sites. As shown in Figure 4, this trend of decreasing z -parameter with increasing β occurs for all the crystals refined here. The fact that this trend is independent of bulk composition provides additional confirmation that the positional disorder at $T(2)$ is not primarily driven by variations in bulk composition, but by local variations in patterns of order at other cation sites in the hydroxide layer.

COMPOSITIONAL COMPLEXITY IN STAUROLITE

The bulk chemical composition of staurolite is essentially the sum of its patterns of local order. Thus having worked our way through the complicated arguments and detailed crystal-chemical analysis, a rather simple picture emerges.

Ideal staurolite

Ideal staurolite has the following atomic arrangement:



For simplicity, we express constituent cations as apfu rather than as site-occupancies. In this structure, $M(3A)$ and $M(3B)$ are on average half-occupied by Al. Where $M(3A) = M(3B) = (Al + \square)$ and $H(1A) = H(1B) = (H_1 + \square_3)$, the structure ideally has orthorhombic symmetry (space group $Ccmm$), with a disordered dis-

tribution of Al over $M(3A)$ and $M(3B)$; where $M(3A) = Al_2$, $M(3B) = \square_2$, $H(1A) = \square_4$ and $H(1B) = H_2 + \square_2$, the structure has monoclinic symmetry (space group $C2/m$), with a fully ordered distribution of cations. There is a continuous variation between these two extremes; this variation can be thought of as an order-disorder series in which the degree of Al - \square order couples to the spontaneous strain (Hawthorne *et al.* 1993b). The table of Pauling bond-strengths for the disordered arrangement (Table 11) shows a perfectly behaved structure with no deviation from ideality.

The resultant formula of this ideal staurolite is $Fe_4^{2+} Al_{18} Si_8 O_{48} H_2$.

Real staurolite

Natural staurolite never even approaches this ideal composition, and the reason for this again seems to be connected with local order. The pattern of local order for this ideal staurolite is shown in Figure 5, assuming for simplicity a fully ordered monoclinic structure [the argument does not change for a disordered (*i.e.*, orthorhombic) structure, but is a little more complicated]. As only one quarter of the $H(1B)$ position is occupied (for the composition $Fe_4^{2+} Al_{18} Si_8 O_{48} H_2$), in one quarter of the patterns it is occupied and in the other three quarters it vacant, as shown diagrammatically in Figure 5. As far as the long-range situation is concerned (Table 11), everything is fine, with ideal bond-strength sums around all the anions. However, on a local scale, the situation is very different. With $M(3A)$ fully occupied, O(1A) is ideally satisfied (Table 12), and there are two local configurations involving occupancy and vacancy of $H(1B)$. Where $H(1B)$ is vacant, the bond-strength sum around O(1B) is 1.5 v.u.; where $H(1B)$ is occupied, the corresponding sum is 2.5 v.u. In neither case is the short-range situation very satisfactory. If $H(1B)$ is occupied, the bond-strength excess can be alleviated by the formation of strong hydrogen bonds with O(3) (see Table 2); the need for this hydrogen bonding can be created by the substitution of lower-valence cations in the "kyanite" layer of the structure: Mg for Al at $M(1)$ and $M(2)$, Al for Si at $T(1)$, and also Mg for Al in the $M(3)$ chain. Consequently, there is a synergistic interaction

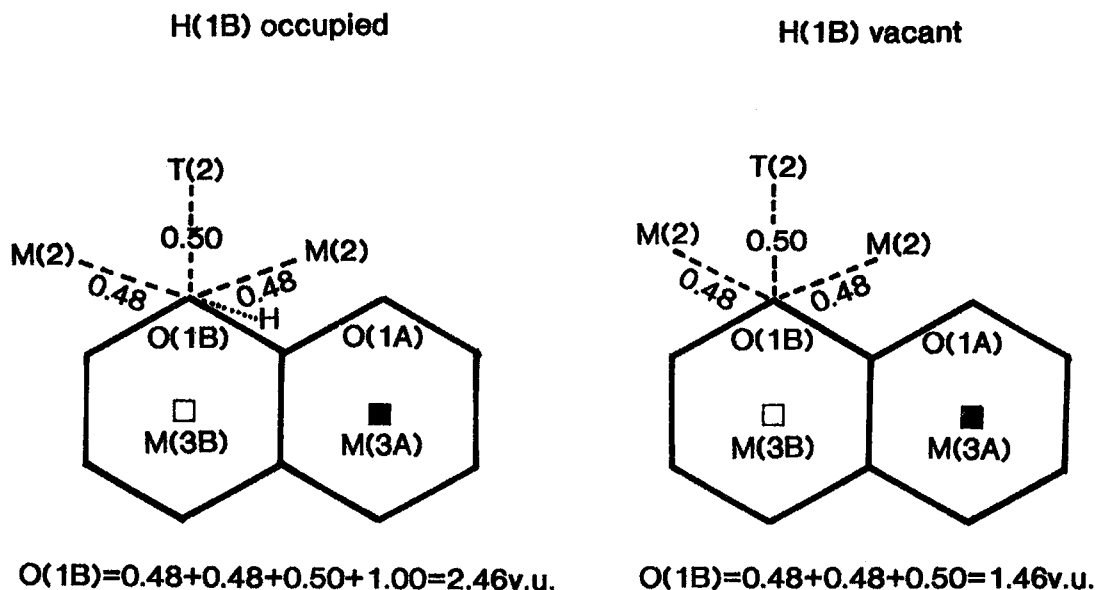


FIG. 5. Diagrammatic representation of patterns of local order in ideal staurolite, for the arrangements in which $M(3A)$ is occupied and $M(3B)$ is vacant.

between these substitutions and the need to satisfy local bond-valence requirements in the oxide-hydroxide layer. Conversely, there is no such mechanism for the relief of the alternate situation where $H(1B)$ is vacant; there seems no simple way of satisfying the local $O(1B)$ bond-valence deficiency if $H(1B)$ does not contribute to its incident bond-valence. A simple way to satisfy this problem is to introduce an additional

two hydrogen atoms at $H(1B)$, whereupon the local bond-valence situation is now stable (see Table 6 for the corresponding bond-valence table). This is satisfactory at the local scale, but produces a long-range excess in charge: $Fe_4^{2+} Al_{18} Si_8 O_{48} H_4$ with a net charge of 2+. Of course, such a stoichiometry cannot be stable, but it is notable that all of the important substitutions in staurolite ($Al \rightarrow Si, Mg \rightarrow Al, M^{(4)}Fe^{2+} +$

TABLE 12. PAULING BOND-STRENGTHS* FOR SCHEMES OF LOCAL ORDER WITH THE $M(3A)$ SITE OCCUPIED IN IDEAL STAUROLITE*

	M(1A)	M(1B)	M(2)	T(1)	M(3A)	M(3B)	M(4A)	M(4B)	T(2)	H(1A)	H(1B)	H(2A)	H(2B)	Sum
O(1A)			$1/2^{2+}$		$1/2^{2+}$		-	-	$1/2$	-	-	-	-	2.0
O(1B)			$1/2^{2+}$			-			$1/2$		-	-	-	1.5
O(2A)	$1/2^{2+}$		$1/2$	1										2
O(2B)		$1/2^{2+}$	$1/2$	1										2
O(3)			$1/2$	1	$1/2^{2+}$		-							2
O(4)	$1/2^{2+}$	$1/2^{2+}$		1										2
O(5)	$1/2^{2+}$	$1/2^{2+}$	$1/2$					-	$1/2^{2+}$					2
Sum	3	3	3	4	3.0	-	-	-	2	1	-	-	-	

	M(1A)	M(1B)	M(2)	T(1)	M(3A)	M(3B)	M(4A)	M(4B)	T(2)	H(1A)	H(1B)	H(2A)	H(2B)	Sum
O(1A)			$1/2^{2+}$		$1/2^{2+}$		-	-	$1/2$	-	-	-	-	2.0
O(1B)			$1/2^{2+}$			-			$1/2$		1	-	-	2.5
O(2A)	$1/2^{2+}$		$1/2$	1										2
O(2B)		$1/2^{2+}$	$1/2$	1										2
O(3)			$1/2$	1	$1/2^{2+}$		-							2
O(4)	$1/2^{2+}$	$1/2^{2+}$		1										2
O(5)	$1/2^{2+}$	$1/2^{2+}$	$1/2$					-	$1/2^{2+}$					2
Sum	3	3	3	4	3.0	-	-	-	2	-	1	-	-	

* there are two corresponding patterns with $M(3B)$ occupied, and $H(1A)$ either occupied or vacant.

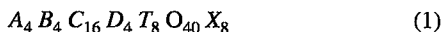
$2T(2)\square \rightarrow M(4)\square + 2T(2)Fe^{2+}$, $\square \rightarrow H, Li \rightarrow Fe^{2+}$) reduce the aggregate charge of the overall structure. Thus we see the chemical complexity of staurolite as the result of competing short-range and long-range bond-valence and electroneutrality requirements of the structure: *the extensive chemical substitutions occur to dissipate a strong local instability in bond-valence distribution.*

STAUROLITE:
STOICHIOMETRY AND END MEMBERS

It is at last apparent from the discussion of the previous section that staurolite is a well-behaved stoichiometric mineral with well-defined end-member compositions.

The chemical formula of staurolite

Following normal usage in complex rock-forming silicate minerals, we could write the general formula for staurolite as the sum of the available occupied sites in the structure:

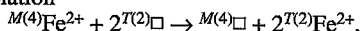


where

$A = Fe^{2+}, Mg, \square (\square \geq 2 \text{ pfu})$	$M(4A), M(4B)$
$B = Fe^{2+}, Zn, Co, Mg, Li,$ $Al, Mn^{2+}, Fe^{3+}(?), \square$	$T(2)$
$C = Al, Fe^{3+}, Cr, V, Mg, Ti$	$M(1A), M(1B), M(2)$
$D = Al, Mg, \square (\square \geq 2 \text{ pfu})$	$M(3A), M(3B)$
$T = Si, Al$	$T(1)$
$X = OH, F, O^{2-}$	$O(1A), O(1B)$

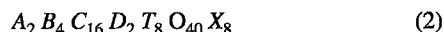
Note that we have separated the *A* group (principal species Fe^{2+} and \square) from the *B* group, and the *D* group (principal species Al and \square) from the *C* group. We have done this to emphasize the fact that both the *A* and the *C* groups have extensive vacancy content (whereas the other groups have only minor or zero vacancy content), and also that the sites corresponding to these two groups are involved in extensive cation-vacancy ordering. As a description of the crystal structure, this is a good formula; as a description of the composition of staurolite, it is not quite as satisfactory. The reason for this involves the *A* and *D* groups and the crystal-chemical limitations on their complete occupancy.

As we have seen above, the occupancy of the *M*(4) sites is related to the occupancy of the *T*(2) site *via* the relation



As the *M*(4) and *T*(2) sites are of corresponding equi-point rank, it can be seen that the total cation content of the *M*(4) site(s) can only reach one-half the total cation content of the *T*(2) site. Thus the *T*(2) site [= *B*-group cations] can be fully occupied (with 4 cations

pfu), whereas the *M*(4) site(s) [= *A*-group cations] can only reach one-half occupancy (with 2 cations pfu). Similarly, the cation population of the *M*(3) site(s) [= *D*-group cations] cannot exceed 2 pfu because of the bond-valence requirements of the *O*(3) anion(s). Indeed, our structural results indicate that the *M*(3) sites have exactly 2.0 apfu (Al and Mg), except for hydrogen-rich staurolite, in which the total falls slightly below this value. Thus summing the site-populations of *M*(1), *M*(2), and *M*(3) never gives a total significantly in excess of 18 apfu (we examined the original hand-sample from which the Zn-rich staurolite of von Knorring *et al.* (1979) was taken, but were unsuccessful in finding a crystal of staurolite). Thus it could be argued that the formula of staurolite should be written as



as then we can define end members with no vacancies at the *A* and *D* groups. However, we feel that this approach is rather deceiving; staurolite is an order-disorder series, and compositions of the form of (2) (*e.g.*, $\square_2 Fe^{2+} Al_{16} Al_2 Si_8 O_{40} [(OH)_2 O_6]$) can be ordered *or* disordered, depending on their position within the series. On the other hand, if we use the formula shown in (1), we can distinguish between ordered and disordered end-member compositions as shown below.

Ordered: $[Fe^{2+}\square]_2 \square_4 Al_{16} [Al_2\square]_2 Si_8 O_{40} [(OH)_6 O_2]$
Disordered: $[(Fe^{2+},\square)_2(\square,Fe^{2+})_2] \square_4 Al_{16} [(Al,\square)_2(\square,Al)_2] Si_8 O_{40} [(OH)_6 O_2]$.

Thus we prefer the formula (1) as written above, with the added information that $\square \geq 2$ pfu at the *A* and *D* groups. Note that the anion total *X* is given as 8 apfu, despite the fact that staurolite has a maximum observed hydrogen-content of 4.2 apfu. This is because there are two sites involved in an $OH^- \rightarrow O^{2-}$ substitution, and from this point of view, the total possible variation is in the range 0–8 apfu, even though such a variation is never (as yet) observed. The formula is no more complex than those of several other rock-forming silicates, and compositional variations are much more restricted than is generally the case.

Principal mechanisms of substitution

The principal heterovalent substitutions in staurolite are as follows:

- | | |
|--|--------------------|
| (1) $\square \rightarrow H$ | $H(1), H(2)$ |
| (2) $M(4)Fe^{2+} + 2T(2)\square \rightarrow$
$M(4)\square + 2T(2)Fe^{2+}$ | $M(4), T(2)$ |
| (3) $\square \rightarrow Al$ | $M(3)$ |
| (4) $Al \rightarrow Si$ | $T(1)$ |
| (5) $Mg \rightarrow Al$ | $M(1), M(2), M(3)$ |
| (6) $Li \rightarrow Fe^{2+}$ | $T(2)$ |

where the arrow indicates that the species on the left is replacing the species on the right.

Each one of these substitutions reduces the charge at the sites at which the substitution occurs. Obviously, the degree to which each substitution occurs is a function of the bulk composition of the rock and the conditions of crystallization or equilibration. Nevertheless, we see a unifying theme here: the local ordering tends to favor a bulk chemistry that is not electrostatically neutral; the principal substitutions all tend to reduce the overall net charge of the formula unit, with the sum of the reductions tending toward 2 for the locally ideal $[\text{Fe}_4 \text{Al}_{18} \text{Si}_8 \text{O}_{48} \text{H}_4]^{2+}$ formula unit.

Principal end-members

The following end-member compositions can be derived from the above staurolite formula and the principal heterovalent substitutions given above:

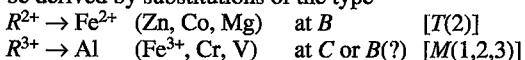
- (1) $\square_4 \text{Fe}_4^{2+} \text{Al}_{16} (\text{Al}_2 \square_2) \text{Si}_8 \text{O}_{40} [(\text{OH})_2 \text{O}_6]$
- (2) $(\square_2 \text{Fe}_2^{2+}) \square_4 \text{Al}_{16} (\text{Al}_2 \square_2) \text{Si}_8 \text{O}_{40} [(\text{OH})_6 \text{O}_2]$
- (3) $\square_4 \text{Fe}_4^{2+} \text{Al}_{16} \square_4 \text{Si}_8 \text{O}_{40} [(\text{OH})_8]$
- (4) $\square_4 \text{Fe}_4^{2+} \text{Al}_{16} (\text{Al}_2 \square_2) (\text{Si}_4 \text{Al}_4) \text{O}_{40} [(\text{OH})_6 \text{O}_2]$
- (5) $\square_4 \text{Fe}_4^{2+} \text{Al}_{16} (\text{Al}_{12} \text{Mg}_4) (\text{Al}_2 \square_2) \text{Si}_8 \text{O}_{40} [(\text{OH})_6 \text{O}_2]$
- (6) $\square_4 \text{Li}_4 \text{Al}_{16} (\text{Al}_2 \square_2) \text{Si}_8 \text{O}_{40} [(\text{OH})_6 \text{O}_2]$

Thus the compositional variations in staurolite are not as intrinsically complicated as those of some other

rock-forming silicate groups (e.g., amphiboles, micas). Nevertheless, they have been difficult to unravel because

- (i) the compositional range of staurolite is very limited compared to such minerals as pyroxenes, amphiboles and micas, and the principal substitutions are less easy to identify;
- (ii) the principal compositional variations (variation in hydrogen and lithium) are "invisible" to the electron microprobe;
- (iii) one particular substitution (2) can be understood only once the associated mechanism of local order is apparent from the site populations derived from crystal-structure refinement.

Homovalent equivalents of these end-members can be derived by substitutions of the type



In addition, other heterovalent substitutions do occur, specifically involving Ti^{4+} and the introduction of Al to the T(2) site; the latter is given by



whereas the details of the Ti^{4+} substitution are not clear (as is usually the case in rock-forming silicate minerals). Note that these latter heterovalent substitutions both tend to *increase* the net positive charge on the mineral. Thus one does not expect considerable amounts of Ti^{4+} or ^BAl in staurolite, as the principal substitutions occur in staurolite to decrease rather than to increase the net charge. This is in fact the case for Ti. Staurolite is never Ti-rich (cf. Ward 1984); Ti rarely exceeds 0.15 apfu, an extremely small amount

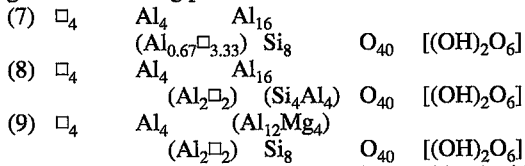
TABLE 13. END MEMBERS AND IMPORTANT EXCHANGE-VECTORS IN STAUROLITE

		End member		exchange vector	
Heterovalent exchanges involving hydrogen					
(1)	\square_4	Fe_4^{2+}	Al_{16}	$(\text{Al}_2 \square_2)$	$\text{Si}_8 \text{O}_{40} (\text{OH})_2 \text{O}_6$
(2)	$(\square_2 \text{Fe}_2^{2+})$	\square_4	Al_{16}	$(\text{Al}_2 \square_2)$	$\text{Si}_8 \text{O}_{40} (\text{OH})_6 \text{O}_2$
(3)	\square_4	Fe_4^{2+}	Al_{16}	(\square_4)	$\text{Si}_8 \text{O}_{40} (\text{OH})_8 \text{O}_3$
(4)	\square_4	Fe_4^{2+}	Al_{16}	$(\text{Al}_2 \square_2)$	$(\text{Si}_4 \text{Al}_4) \text{O}_{40} (\text{OH})_6 \text{O}_2$
(5)	\square_4	Fe_4^{2+}	Al_{16}	$(\text{Al}_{12} \text{Mg}_4)$	$(\text{Al}_2 \square_2) \text{Si}_8 \text{O}_{40} (\text{OH})_6 \text{O}_2$
(6)	\square_4	Li_4	Al_{16}	$(\text{Al}_2 \square_2)$	$\text{Si}_8 \text{O}_{40} (\text{OH})_6 \text{O}_2$
Heterovalent exchanges involving ^BAl					
* (7)	\square_4	Al_4	Al_{16}	$(\text{Al}_{0.67} \square_{3.33})$	$\text{Si}_8 \text{O}_{40} (\text{OH})_2 \text{O}_6$
(8)	\square_4	Al_4	Al_{16}	$(\text{Al}_2 \square_2)$	$(\text{Si}_4 \text{Al}_4) \text{O}_{40} (\text{OH})_2 \text{O}_6$
(9)	\square_4	Al_4	$(\text{Al}_{12} \text{Mg}_4)$	$(\text{Al}_2 \square_2)$	$\text{Si}_8 \text{O}_{40} (\text{OH})_2 \text{O}_6$
Homovalent exchanges					
(1)	\square_4	Zn_4	Al_{16}	$(\text{Al}_2 \square_2)$	$\text{Si}_8 \text{O}_{40} (\text{OH})_2 \text{O}_6$
(2)	\square_4	Co_4	Al_{16}	$(\text{Al}_2 \square_2)$	$\text{Si}_8 \text{O}_{40} (\text{OH})_2 \text{O}_6$
(3)	\square_4	Mg_4	Al_{16}	$(\text{Al}_2 \square_2)$	$\text{Si}_8 \text{O}_{40} (\text{OH})_2 \text{O}_6$
(4)	\square_4	Fe_4^{2+}	Fe_{16}^{3+}	$(\text{Fe}_2^{3+} \square_2)$	$\text{Si}_8 \text{O}_{40} (\text{OH})_2 \text{O}_6$

* note that the end member could be simplified to $\square_4 \text{Al}_4 \text{Al}_{16} \square_4 \text{Si}_8 \text{O}_{40} [(\text{OH})_2 \text{O}_6]$ at the expense of complicating the exchange vector: $\text{Al}_4 \square_4 (\text{OH})_2 [(\text{Fe}_2^{3+} \text{Al}_2 \text{O}_2)]_{-1}$.

compared with other rock-forming silicates [*e.g.*, amphiboles: Leake (1968), pyroxenes: Deer *et al.* (1982), vesuvianite: Groat *et al.* (1992).

Al may be incorporated into the *T*(2) tetrahedron by several different substitutions, using the formula $\square_4 \text{Fe}^{2+}_4 \text{Al}_{18} \text{Si}_8 \text{O}_{40} (\text{OH})_2 \text{O}_6$ as a basis. It can be combined with various charge-reducing substitutions to give the following possible end-members:



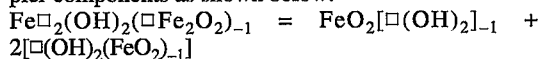
Note that end-member (7) could be combined with a substitution of the type $\square\text{H}_3(\text{Al}\square)_1$ to give the more ordered form: $\square_4\text{Al}_4\text{Al}_{16}\square_4\text{Si}_8\text{O}_{40}[(\text{OH})_4\text{O}_4]$. The relative importance of these substitutions and end-members [and other possible schemes involving Al at *T*(2)] is difficult to judge because of the problems associated with deriving ^BAl contents in staurolite, and because the amount of ^BAl is usually quite small.

Vector representation of staurolite compositions

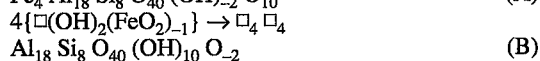
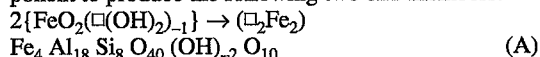
The vector method of representing mineral compositions is quite widely used at present, and a brief description of staurolite chemistry in these terms is warranted. Explanations and applications of the method of vector representation in this context are given by Burt (1979) and Thompson (1982).

An important aspect of this type of representation is the choice of the additive component. From an algebraic point of view, any of the proposed end-members could be used. However, our identification of an ideal staurolite (see above), together with the arguments concerning the role of the various important substitutions, indicate that the most appropriate additive component is $\square_4 \text{Fe}^{2+} \text{Al}_{18} \text{Si}_8 \text{O}_{40} (\text{OH})_2 \text{O}_6$. The various end-members can then be derived from this using the appropriate exchange-vectors. The end-members discussed above, together with their related exchange-vectors, are listed in Table 13.

The exchange vector $\text{Fe}\square_2(\text{OH})_2(\square\text{Fe}_2\text{O}_2)_{-1}$ associated with end-member (2) requires some discussion. This is quite a complex substitution, and the associated exchange-vector can be resolved into two simpler components as shown below:



These exchange operators act on the additive component to produce the following two end-members:



From an algebraic point of view, these are perfectly adequate end-members, and can be used as such to

represent compositional variations. However, from a crystal-chemical viewpoint, these operators must couple together in the manner indicated above, as deviation from this relationship produces physically impossible crystal structures. End-member (A) would have Fe-Fe separations of 1.65 Å, a physical and chemical impossibility in such a structure; end-member (B) would have unacceptable bond-valence sums about the O(5) anion. Thus for simplicity and for crystal-chemical reasons, we prefer to use the more complicated exchange-vector (2) in Table 13.

The homovalent exchange-vectors (Table 13) are quite straightforward if it is understood that these also may combine with heterovalent exchange vectors, with a change in the coordination number of the relevant exchange-components.

COMPOSITIONAL VARIATIONS IN NATURAL STAUROLITE

The restricted nature of some of the chemical variations in staurolite should make the graphical representation of major compositional variations reasonably straightforward. Unfortunately, two of the principal compositional variables (hydrogen and lithium) are rarely measured. The third principal variable is a local order-disorder-related substitution that (in the absence of a crystal-structure refinement) can only be partly assessed from the sum of the cations, which in turn can only be calculated correctly if the concentrations of hydrogen and lithium are determined. Moreover, the variable aggregate occupancy of the *M*(3) site also contributes to the variation in the sum of the cations, and this can only be assessed from a crystal-structure refinement. From a crystal-chemical viewpoint, substitutions (2) and (3) are distinct. However, they are the only substitutions that reduce the cation sum below its ideal value of 30 apfu; thus a pragmatic approach to representing chemical variations in the absence of a crystal-structure refinement is to combine these two substitutions and use the sum of the cations as a measure of their extent. Even if this is done, the number of fully analyzed samples available for examination is low; we are essentially restricted to the high-quality analytical results of Holdaway *et al.* (1986b).

Vector representation of natural compositions

The most important exchange-vectors in terms of compositional variation in staurolite are (2) and (6) (Table 13). This is not to say that the other exchange vectors are unimportant; however, the extent of the compositional variations in these other directions is minor by comparison [*i.e.*, for (4) and (5)]. Compositional variations in staurolite can usefully be considered in three dimensions. The mean Si content of the staurolite samples of Holdaway *et al.* (1986b) is 7.65 apfu; the mean ¹⁶Mg content of the subset of

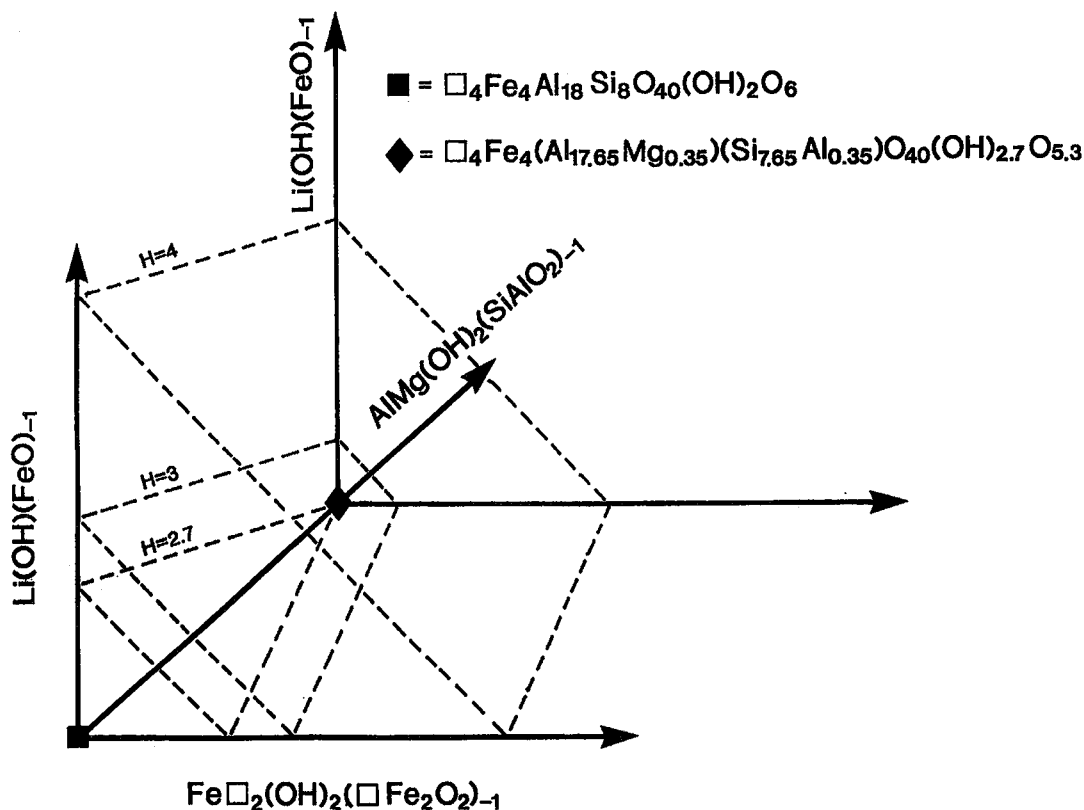


FIG. 6. Idealized compositional space for staurolite defined by the additive component $\square_4\text{Fe}_4\text{Al}_{18}\text{Si}_8\text{O}_{40}(\text{OH})_2\text{O}_6$ and the exchange vectors $\text{Fe}\square_2(\text{OH})_2(\square\text{Fe}_2\text{O}_2)_{-1}$, $\text{Li}(\text{OH})(\text{FeO})_{-1}$ and $\text{AlMg}(\text{OH})_2(\text{SiAlO}_2)_{-1}$; the space is also contoured for various values of H content. The point along the $\text{AlMg}(\text{OH})_2(\text{SiAlO}_2)_{-1}$ vector at $H = 2.7$ apfu has the formula indicated on the figure, and serves as a useful origin for a two-dimensional representation of natural compositions in staurolite.

those samples examined by Hawthorne *et al.* (1993a) is 0.36 apfu. This suggests that we can combine exchange vectors (4) and (5) according to the scheme indicated below

$\text{Mg}(\text{OH})(\text{AlO})_{-1} + \text{Al}(\text{OH})(\text{SiO})_{-1} = \text{MgAl}(\text{OH})_2(\text{SiAlO}_2)_{-1}$ and represent staurolite compositions in the space shown in Figure 6; note that this space can easily be contoured for (OH) content, although it does ignore exchange vector (3).

A further simplification can be introduced in the following way. In terms of the ^{6}Mg and $^{T(1)}\text{Al}$ contents, natural samples of staurolite quite closely approximate the composition $(\text{Al}_{17.65}\text{Mg}_{0.35})(\text{Si}_{7.65}\text{Al}_{0.35})$; this composition is marked on the $\text{MgAl}(\text{OH})_2(\text{SiAlO}_2)_{-1}$ axis of Figure 6. If we draw a plane through this point orthogonal to the $\text{MgAl}(\text{OH})_2(\text{SiAlO}_2)_{-1}$ vector, we may project the compositions of natural samples of staurolite onto this plane with a minimum of relative spatial distortion; this is shown in Figure 7. There is some error in the apparent (OH) contents because we have ignored sub-

stitution (3), ^{6}Mg is not exactly the same as $^{T(1)}\text{Al}$ (and also possibly because of more minor heterovalent substitutions involving Ti or $^{T(2)}\text{Al}$); thus the hydrogen-rich staurolite compositions project onto the $H \approx 4.3$ apfu contour rather than the $H \approx 4.15$ apfu contour. Nevertheless, the compositional variations are quite well represented by this projection.

Not surprisingly, there is a correlation between H-content and total number of cations, essentially the variation due to substitutions (2) and (3). This is examined in more detail in Figure 8 for the complete chemical analytical data-set of Holdaway *et al.* (1986b). Here we see a well-developed inverse correlation between cation sum and hydrogen content, a relationship that is perturbed by the presence of Li; multiple regression analysis gives the relationship

$$\text{CATSUM} = 31.333 - 0.495(22) H + 0.321(38) \text{Li} \quad R = 0.974$$

Where lithium is absent, the cation sum would be 30 for a hydrogen content of 2.69 apfu; for $H = 4$ apfu

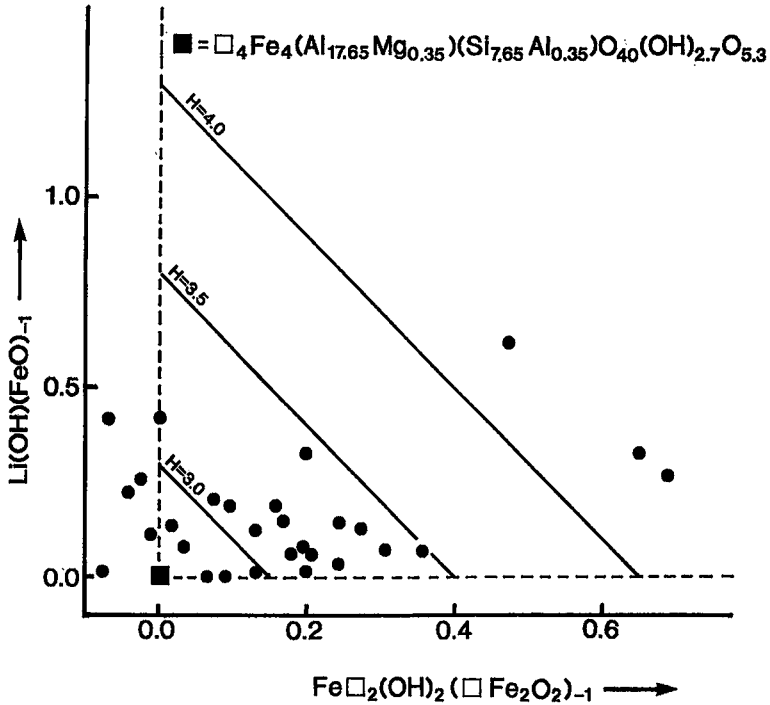


FIG. 7. Two-dimensional compositional space for staurolite, showing the staurolite samples of Holdaway *et al.* (1986b); the figure is contoured for H content.

(and Li = 0), the cation sum would be 29.35 apfu; for a cation sum of 29, the hydrogen content would be 4.71 apfu. These numbers agree quite well with the projection of Figure 8.

Chemical correlations involving Mg

It is apparent from the results of Hawthorne *et al.* (1993a) that Mg has several very different roles in the

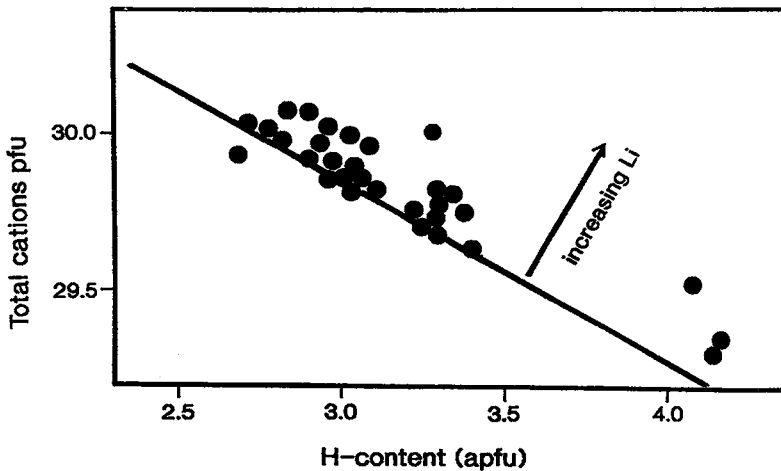


FIG. 8. Variation in H content with varying cation sum (CATSUM) of the formula unit; note that displacement to the upper right correlates with increasing Li content.

staurolite structure; the relative importance of these roles varies with bulk composition. In common (Fe-rich) staurolite, approximately one-half of the Mg occupies the $M(1,2,3)$ sites, and one-half occupies the $T(2)$ site. In Mg-rich staurolite, Mg occupies $M(1,2,3)$ in absolute amounts (not relative amounts) comparable to normal staurolite, the remainder occupying both $T(2)$ and $M(4)$. Hence we do not expect simple diadochy between Mg and any other chemical component (e.g., Fe), perhaps explaining the controversy surrounding the behavior of Mg in staurolite.

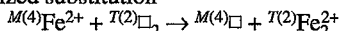
Mg in Li-free staurolite: It is apparent from the above discussion that Mg has at least two roles in staurolite. It may be involved in simple $Mg \leftrightarrow Fe^{2+}$ substitution, either [4]-coordinate at the $T(2)$ site or [6]-coordinate at the $M(4)$ sites (or both). This type of substitution has been the generally accepted one, particularly in synthesis studies. However, Mg also is involved in substitution for Al at the $M(1,2,3)$ sites: the $Mg(OH)(AlO)_{-1}$ exchange-vector. This is in line with the findings of Griffen & Ribbe (1973) and Griffen *et al.* (1982), who proposed that (Al + Zn) are the principal substituents for Fe at $T(2)$, and that most (if not all) Mg occurs at the $M(3)$ sites. The results of the present work show that both proposals are partly correct (*cf.* Enami & Zang 1989): Mg substitutes for Fe^{2+} at $T(2)$ and for Al at $M(1,2,3)$. In addition, natural occurrences indicate that pressure favors the former substitution.

Mg in Li-bearing staurolite: Examination of the bond-valence arrangements for patterns of local order involving Li (Table 9) shows that most of the anions have small to significant deficiencies in their bond-valence sums. This fact suggests that local configurations involving Li will not favor $^{[6]}Mg \rightarrow ^{[6]}Al$ substitution, as this will decrease the bond-valence sums around the anions even further. This situation does seem to be the case for the crystals of Li-rich staurolite examined by Hawthorne *et al.* (1993a), and perhaps accounts for the negative correlation between Li and $Mg/(Fe+Mg)$ observed by Dutrow *et al.* (1986).

SUMMARY

1. The chemical complexity of staurolite results from the interaction between long-range and short-range charge-balance requirements.

2. Of particular importance with regard to local ordering and (long-range) electroneutrality is the hitherto unrecognized substitution

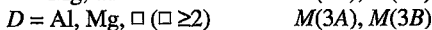
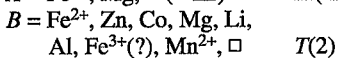
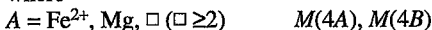


which reduces the net charge and the total number of cations in the structure while maintaining an ideal local bond-valence distribution.

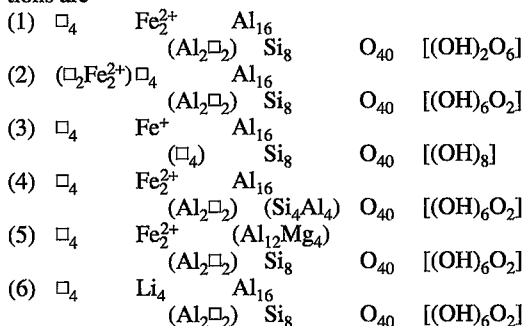
3. The chemical composition of staurolite can be written as



where



4. The principal (heterovalent) end-members compositions are



Homovalent end-members can be derived from these by the usual type of substitutions (*i.e.*, $Zn \rightarrow Fe^{2+}$, $Co^{2+} \rightarrow Fe^{2+}$, $Mg \rightarrow Fe^{2+}$).

5. The exchange vectors corresponding to these end-members are as follows:

- (1) Additive component
- (2) $Fe\square_2(OH)_2(\square Fe_2O_2)_{-1}$
- (3) $\square_2(OH)_6(Al_2O_6)_{-1}$
- (4) $Al(OH)(SiO)_{-1}$
- (5) $Mg(OH)(AlO)_{-1}$
- (6) $Li(OH)(FeO)_{-1}$

6. The compositional variations in natural staurolite can be reasonably well represented in the space $Fe\square_2(OH)_2(\square Fe_2O_2)_{-1} - Li(OH)(FeO)_{-1} - MgAl(OH)_2(SiAlO_2)_{-1}$ but this representation does require site populations derived from crystal-structure refinement.

7. Exchange vectors (2) and (3) cause a decrease in the sum of the cations (CATSUM) per formula unit. Where only chemical data are available, the principal (heterovalent) chemical variables are CATSUM, H and Li contents.

ACKNOWLEDGEMENTS

We thank the referees for their thoughtful comments. The CNR Centro di Studio per la

Cristallochimica e la Cristallografia, Pavia, was a sanctuary from the cold hard world during the course of this work. Financial support was provided by the Natural Sciences and Engineering Research Council of Canada, CNR-NATO and a Killam Fellowship to FCH.

REFERENCES

- ALEXANDER, V.D. (1989): Iron distribution in staurolite at room and low temperatures. *Am. Mineral.* **74**, 610-619.
- BROWN, I.D. (1976a): On the geometry of O-H...O hydrogen bonds. *Acta Crystallogr.* **A32**, 24-31.
- (1976b): Hydrogen bonding in perchloric acid hydrates. *Acta Crystallogr.* **A32**, 786-792.
- (1981): The bond-valence method: an empirical approach to chemical structure and bonding. In *Structure and Bonding in Crystals II* (M. O'Keeffe & A. Navrotsky, eds.). Academic Press, New York (1-30).
- & ALTERMATT, D. (1985): Bond-valence parameters obtained from a systematic analysis of the inorganic crystal structure database. *Acta Crystallogr.* **B41**, 244-247.
- BURT, D.M. (1979): Exchange operators, acids and bases. In *Problems in Physico-Chemical Petrology 2* (V.A. Zharikov, W.I. Fonarev & S.P. Korikovskiy, eds.). Nauka Press, Moscow (in Russ.; 3-15).
- DEER, W.A., HOWIE, R.A. & ZUSSMAN, J. (1982): *Rock-Forming Minerals. 1A. Orthosilicates*. Longmans, Green and Co., London, U.K.
- DUTROW, B.L., HOLDAWAY, M.J. & HINTON, R.W. (1986): Lithium in staurolite: its petrologic significance. *Contrib. Mineral. Petrol.* **94**, 496-506.
- DYAR, M.D., PERRY, C.L., REBBERT, C.R., DUTROW, B.L., HOLDAWAY, M.J. & LANG, H.M. (1991): Mössbauer spectroscopy of synthetic and naturally occurring staurolites. *Am. Mineral.* **76**, 27-41.
- ENAMI, M. & ZANG, QILIA (1989): Magnesian staurolite in garnet-coriundum rocks and eclogite from the Donghai district, Jiangsu province, east China. *Am. Mineral.* **73**, 48-56.
- GRIFFEN, D.T., GOSNEY, T.C. & PHILLIPS, W.R. (1982): The chemical formula of natural staurolite. *Am. Mineral.* **67**, 292-297.
- & RIBBE, P.H. (1973): The crystal chemistry of staurolite. *Am. J. Sci.* **273-A**, 479-495.
- GROAT, L.A., HAWTHORNE, F.C. & ERCIT, T.S. (1992): The chemistry of vesuvianite. *Can. Mineral.* **30**, 19-48.
- HAWTHORNE, F.C., UNGARETTI, L., OBERTI, R., CAUCIA, F. & CALLEGARI, A. (1993a): The crystal chemistry of staurolite. I. Crystal structure and site populations. *Can. Mineral.* **31**, 551-582.
- , ——, ——, —— & —— (1993b): The crystal chemistry of staurolite. II. The orthorhombic → monoclinic phase transition. *Can. Mineral.* **31**, 583-595.
- HOLDAWAY, M.J., DUTROW, B.L., BORTHWICK, J., SHORE, P., HARMON, R.S. & HINTON, R.W. (1986a): H content of staurolite as determined by H extraction line and ion microprobe. *Am. Mineral.* **71**, 1135-1141.
- , —— & SHORE, P. (1986b): A model for the crystal chemistry of staurolite. *Am. Mineral.* **71**, 1142-1159.
- VON KNORRING, R., SAHAMA, T.G. & SIVOLA, J. (1979): Zincian staurolite from Uganda. *Mineral. Mag.* **43**, 446.
- LAGER, G.A., ARMBRUSTER, T. & FABER, J. (1987): Neutron and x-ray diffraction study of hydrogarnet $\text{Ca}_3\text{Al}_2(\text{O}_4\text{H}_4)_3$. *Am. Mineral.* **72**, 756-765.
- LEAKE, B.E. (1968): A catalog of analyzed calciferous amphiboles together with their nomenclature and associated minerals. *Geol. Soc. Am., Spec. Pap.* **98**.
- SHANNON, R.D. (1976): Revised effective ionic radii and systematic studies of interatomic distances in halides and chalcogenides. *Acta Crystallogr.* **A32**, 751-767.
- SMITH, J.V. (1968): The crystal structure of staurolite. *Am. Mineral.* **53**, 1139-1155.
- STÄHL, K., KVICK, Å. & SMITH, J.V. (1988): A neutron diffraction study of hydrogen positions at 13K, domain model, and chemical composition of staurolite. *J. Sol. State Chem.* **73**, 362-380.
- THOMPSON, J.B., JR. (1982): Composition space: an algebraic and geometric approach. In *Characterization of Metamorphism through Mineral Equilibria* (J.M. Ferry, ed.). *Rev. Mineral.* **10**, 1-31.
- WARD, C.M. (1984): Titanium and the color of staurolite. *Am. Mineral.* **69**, 541-545.

Received May 26, 1993, revised manuscript accepted November 5, 1993.